ABSTRACT

SEGREGATION AND FLOW CHARACTERIZATION IN VIBRATED HOPPER

by
Thottiam P. Ravichandran

Experiments and numerical simulation studies were carried out on vertically vibrated wedge-type hoppers containing binary mixtures for the present research. The studies focussed on segregation analysis of the hopper discharge and the characterization of flow pattern of the binary mixtures in sealed hoppers, over wide ranges of frequency and amplitude of acceleration to determine the effect of these parameters.

The results of segregation study show that vibration promotes segregation of the binary mixtures. However, increase in frequency was found to make the contents of segregated discharge more uniform. Also, increase in wedge angle seemed to help in reducing segregation.

The experimentally observed flow patterns, showed a new type of four-loop convection pattern. The simulation studies revealed some of the experimental observations. Thus, the experimentally observed patterns included three regimes, namely, an unstable heaping state, symmetrical convection pattern, and unstable region with surface waves.

SEGREGATION AND FLOW CHARACTERIZATION IN VIBRATED HOPPER

by
Thottiam P. Ravichandran

A Master's Thesis
Submitted to the Faculty of
New Jersey Institute of Technology
In Partial Fulfillment of the Requirements for the Degree of
Master of Science in Mechanical Engineering

Department of Mechanical Engineering

January 2000

APPROVAL PAGE

SEGREGATION AND FLOW CHARACTERIZATION IN VIBRATED HOPPER

Thottiam P. Ravichandran

Dr. Rajesh N. Dave, Thesis Advisor — Date
Professor of Mechanical Engineering, NJIT

Dr. Moinuddin Malik, Committee Member — Date
Visiting Professor of Mechanical Engineering, NJIT

Dr. Chao Zhu, Committee Member — Date
Assistant Professor of Mechanical Engineering, NJIT

BIOGRAPHICAL SKETCH

Author: Thottiam P. Ravichandran

Degree: Master of Science in Mechanical Engineering

Date: January 2000

Undergraduate and Graduate Education:

- Master of Science in Mechanical Engineering,
  New Jersey Institute of Technology,
  Newark, New Jersey, 2000

- Bachelor of Science in Mechanical Engineering,
  Regional Engineering College,
  Durgapur, India, 1996

Major: Mechanical Engineering

Presentations and Publications:

T. P. Ravichandran, A. Mujumdar, C.Y. Wu, S.Watano, R.N. Dave "Study of Powder Segregation during Discharge from a Vibrated Hopper," Presented at AIChE 1998 Annual Meeting, November 15-20

T. P. Ravichandran, A. Mujumdar, G. James, R.N. Dave, C.Y. Wu, S. Watano, "Study of Powder Segregation during Discharge from a Vibrated Hopper," Particle Technology Symposium, NJIT, March 25-26,1999.

This thesis is dedicated to my family and friends

ACKNOWLEDGMENT

The author wishes to express his sincere gratitude to his advisor, Dr. Rajesh N. Dave, for his guidance, friendship and moral support throughout this research. The author would like to thank Dr. Moinuddin Malik, Dr. Chang Yu-Wu and Dr. Satoru Watano for many stimulating discussions and for furnishing theoretical predications.

Special thanks to Dr. Rong Chen and Dr. Chao Zhu for serving as members of committee. The author would like to thank his research group colleagues for their support and cooperation during his research. The author is also grateful to Dr. Maher of Rutgers for providing the code, which was modified for the purpose of these studies.

TABLE OF CONTENTS

Chapter **Page**

TABLE OF CONTENTS
(Continued)

Chapter **Page**

LIST OF TABLES

LIST OF FIGURES

Figure **Page**

LIST OF FIGURES
(Continued)

Figure **Page**

LIST OF FIGURES
(Continued)

Figure **Page**

CHAPTER 1

INTRODUCTION

1.1 Vibration of Bulk Solids

Vibration as a means of agitating bulk of particulate solids is employed in many industries. The industries are of diverse settings such as, chemical, food, material, mineral, pharmaceutical and many others where the solid materials in one or more stages of processing are in particulate form. Vibrating conveyers and feeders, sorting and packing tables, and vibro-fluidized beds are some of the vibration-based devices. The specific tasks of vibration may include fluidization, flow enhancement, segregation, and compaction, among others. However, despite the obvious importance, there is not much in the technical literature that provides guidelines for utilizing vibration to achieve the specific tasks effectively and the methodologies for the design of vibratory devices. This is basically for the reason that the behavior of vibrating particulate materials is not well understood. Consequently, the vibration of bulk solids is an active area of research. Much of the research work in the area has been directed toward flow characterization of vibrating particulate materials through experimental studies. In recent years, due to enormous growth of computing power and computer visualization techniques, computer simulation has become an increasingly popular tool for that purpose.

The research literature on the vibration behavior of particulate solids is extensive, and may be broadly classified into three areas of interest: (1) characterization of particulate behavior inside vibrating beds, vessels, hopper-like containers; (2) effect of vibration on segregation of particulate mixtures of two or more types of particulate solids; and (3) effect of vibration on particulate flows from hoppers. Herein, a brief

review of the literature relevant to the present work is in order. Specifically, the literature being cited is on particulate behavior in vibrated containers and the effect of vibration on segregation in hopper flow.

Historically, the earliest reported studies on vibrating granular beds are related to structural vibrations. In the experimental work reported in 1782, which marks the beginning of research in structural dynamics, Chladni [1] used sand for displaying nodal patterns of completely free vibrating plates. Faraday's work [2], also on elastic vibrations and published in 1831, reported convection and heaping in the flow of particles on vibrated beds. These two characteristics of the solids flows in vibrated beds are still intriguing for researchers and remain quite unexplained.

Studies on the specific problem of vibration of particulate materials began apparently more recently than the two works cited earlier. Bachmann [3] and, later, Kroll [4] made important contribution as their studies were directed toward the effect of depth of bed of granular material. These authors reported that in beds having depths less than six times the particle diameter, vibrations set the particles into a fluidized state. However, in beds of thickness greater than six particle diameters, the particles behave as a single mass. These two works actually considered what are now recognized as shallow and deep beds. The first attempt toward clear characterization of particulate behavior in vibrated beds was made by Thomas et al. [5]. These authors used two-dimensional, rectangular containers and, through their extensive experimental studies, identified four states of particulate behavior in shallow beds; these were referred to as "Newtonian-I," "Newtonian-II," "coherent-expanded," and "coherent-condensed" states. In the Newtonian-I state, the particles are in a state of random motion with nearly uniform

density in vertical direction. The Newtonian-II state appearing with some increase in the bed depth exhibits segregation of two layers during a portion of a cycle: a dilute upper layer of particles in random motion of particles, and dense layer near the bottom. Further increase in the depth results in a transition to coherent-expanded state in which the bed of particles oscillates as single mass but is accompanied by considerable expansion and contraction. Still further increase in depth leads to coherent-condensed state, which represents transition to deep bed regime as observed by Bachmann [3].

It is now widely accepted that the two most important parameters which govern the behavior of particulate materials under vibration are: (1) the dimensionless depth of particulate bed, h_o/d, where h_o and d are the depth of particulate bed and particle diameter d, respectively, and (2) the dimensionless amplitude of acceleration, or simply g-level acceleration, $\Gamma = a\omega^2/g$ where a is amplitude of vibration, ω the angular frequency of vibration, and g is the gravitational acceleration. The behavior of particulates in deep beds exhibits a variety of phenomena; the occurrence of these phenomena depends on the dimensionless depth h_o/d and the g-level acceleration Γ. Wassgren et al. [6] and Wassgren [7] have recently presented a systematic characterization of the deep-bed phenomena. These phenomena, which occur with increasing g-level acceleration, include: cellular convection, heaping, small-amplitude surface waves, arching, and large-amplitude surface waves.

As pointed out earlier, the phenomena of cellular convection and heaping were first observed by Faraday [2]. The cellular convection, which begins at about 1-g acceleration, is exhibited in the form of particles moving along the sidewalls of the container and re-circulating within the bulk of material. The movement of particles is

observed to be downward along vertical walls as in cylindrical containers, and upward along inclined walls as in conical or wedge-type containers. Heaping, which occurs at a slightly higher acceleration of about 1.2 g and accompanies convection, is observed by the formation of a mound of the bulk either centrally placed or more commonly inclined from one end of the container to the other. Cellular convection and heaping have been studied by many researchers; see for example, [6]-[11]. With further increase in the g-level acceleration, convection and heaping phenomena disappear, and a variety of phenomena, such as, small-amplitude surface waves, arching, and large-amplitude have been observed [6, 7], [11]-[13].

Many particulate processes involve mixture of two or more materials. An undesirable outcome of vibration is segregation of constituents from the mixture. For example, in a vibrating container having a binary mixture, segregation is shown by accumulation of larger size particles at the top of smaller size particles. Ahmad and Smalley [14] made systematic investigations on the effect of various parameters on segregation. Experiments were conducted by introducing a large particle at the base of small particles in a cylindrical container. The cylinder was subjected to vertical vibrations and segregation was studied in terms of rise time of the large particle. Among the various parameters considered, the acceleration and size of large particle was found to be the most important; segregation time was found to increase with increase in acceleration or the particle size. Following the work of Ahmad and Smalley, segregation study based on the rise time of a single large size particle has been used by many other researchers, for example, Knight et al. [15], Vanel et al. [16]. Brone and Muzzio [17] utilized an interesting technique for segregation study. In this technique, binary mixture of equal

amounts (by volume) of two different size particles was vibrated in a cylindrical vessel for a specified time. The mixture was subsequently frozen with a binder. Segregation was studied by examining the structure on the surfaces of the vertical slices cut from the frozen mixture. Borne and Muzzio [16] showed that the binary mixture can be driven back and forth between segregated and homogeneous states by decreasing or increasing the vibration frequency.

The theories on the segregation mechanism may be regarded as geometric and convection theories. The geometric theories explain segregation as a consequence of the higher tendency of small particles to fill gaps or holes formed underneath the larger ones [16, 17]. The convection theory proposed by Knight et al. [15], attributes segregation to the formation of convection rolls that tend to carry the larger particles to the bed surface.

The recent developments in the computer hardware of increased processing speeds and data storage capabilities, cost reduction of the hardware, and availability of computer graphics and visualization techniques have made computer simulations a lucrative tool to study the particulate dynamics. By computer simulation one can realize the actual experiment, and can achieve much more than what may not be possible experimentally for many reasons. The simulation can control and aid in the measurement of various parameter which are not feasible in experiments. They can also create an ambience, for example reduced-gravity environment, which it is not possible to do with experiments. Also, the state of particulate motion can be known at all times in simulation.

Most simulation models are discrete element (DE) types in that the particulate bulk is modeled as a system of individual particles, which interact with the other particles only at the contact points. The time step in the DE models is taken to be so small that

during a single time step any disturbances may be considered to propagate no farther than its contacting particles. Among the various versions of the DE simulations, the discrete element method (DEM) developed by Cundal and Strack [18] is most widely used. Another widely used technique advanced by Walton and Braun [19] and Walton [20] is also a DE simulation; however, the contact model of these authors [19, 20] is considerably different from that of Cundal and Strack [18].

Discrete element simulation has been employed for vibrating particulate systems by a number of authors. These include simulation of a variety of phenomena, such as, [7], [21]-[26], heaping [7], and arching [27], and the shallow bed phenomena [28].

1.2 The Present Work

Granular flow is a complex phenomenon, and it is not surprising that its basic mechanics is not well understood. Complexity in the understanding and investigation of granular flows also comes due to an enormous of variables involved which include the shape, size, and materials of the particles, the types of handling devices, environmental conditions, and so on.

The problems in the present research have been undertaken from a rather practical standpoint. The present work is concerned with segregation analysis and particulate flow characterization in vertically vibrated planar wedge-type hopper. Specifically the problems considered in this thesis are the following:

1. Experiments on segregation analysis of discharge of binary mixtures from vertically-vibrated wedge-type hoppers,

2. Experiments on flow characterization of binary mixtures in vertically-vibrated, wedge-type, sealed hoppers, and
3. Numerical simulation of binary-mixture flows in vertically vibrated, wedge-type, sealed hoppers.

In the following chapters of this thesis, the details of numerical simulation technique and its computer code are described in Chapter 2. The details of the experimental facility used for the experimental investigations are given in Chapter 3. The results of the research work on the three aforementioned problems are presented and discussed in Chapter 4. Finally, the conclusions of the investigations are presented in Chapter 5. In this chapter, the possibilities of further research that arise from the present work are also described.

CHAPTER 2

NUMERICAL MODELLING

2.1 The Numerical Simulation Code

The granular dynamic simulation is an apparent forerunner of the granular dynamic simulation. However, the analogy between the two techniques extends to no more than that both consider the dynamical system of particles as a deterministic, classical N-body problem. The molecular and granular systems are essentially different physical systems. The molecules in a fluid are always in a state of random motion, the granules in a bulk solid set in motion through some sustained source of disturbance. Energy conservation is essential for a molecular system where as energy dissipation is the characteristic for the granular system. A part of kinetic energy is lost either in dissipation due to friction and/or plastic deformations in particulate collisions. Interacting solid particles are generally modeled as hard or soft spheres. The hard sphere model considers the particles to be infinitely stiff so that it rebounds immediately after the collision with another particles. The soft sphere model allows colliding particles to overlap a small percentage of their diameters.

The numerical simulation code used in the present study is the C++ version, adapted by Maher Moakher for hopper flows, from the Fortran code developed by O. R. Walton based on the three-dimensional, soft sphere granular dynamics model of Walton and Braun [19]. The present author introduced some modifications to account for the vertical vibrations of the hopper.

The flow chart of the code is given in APPENDIX A. The operation of the code is briefly as follows. The initial coordinates for particle centers are generated via a random

number generator. A radii expansion technique is used to determine a non-overlapping distribution of the particles. The zero-time setting of the particles is configured. This is done by allowing the particles to fall under gravity and settle into a loose packing; this is equivalent to pouring and setting of the granules in the hopper in an actual experiment. The hopper is set in vertical vibration and numerical simulation begins with the solution of the equations of motion of the interacting particles (modeled as soft spheres). The solution is based on a finite difference algorithm of Verlet [30] which carries out integration of the equations of motion in discrete time steps.

The code comprises of a number of functions (or subroutines). The input parameters needed for simulation are read in the function **datain**. These parameters are as follows:

- Types of (spherical) particles in the granular mixture
- Number of each type of particles
- Diameter and mass of each type of particle
- Coefficients of restitution (particle/particle and particle/wall)
- Friction coefficients (particle/particle and particle/wall)
- Stiffness coefficients (particle/particle and particle/wall)
- Ratio of normal to the tangential force
- Hopper dimensions
- Maximum simulation time
- Gravity acceleration
- Frequency and g-level acceleration of hopper vibration

For a numerical simulation beginning at zero time, the initial positions and velocity of the particles are generated in the function **init1**. However, if it is a continuation of an earlier simulation, the function **init2** is called which reads the end conditions of the earlier simulation, and sets them as the initial conditions of the current simulation. The initial configuration is completed after the **findrad** is executed. The inter-particle forces are calculated, using the Walton-Braun model [19], in the function **forces**. The forces are utilized to determine displacements and velocities by integrating the equations of motion in the function **integ**.

In the following, salient features of the simulation code and the model are described.

2.2 Initial Condition Generation

After the simulation parameters are read in the function **datain**, the particles are assigned center coordinates using a random number generator in the function **init1**. For this purpose, the hopper space is divided into a number of layers which equal the number of types of particles in the granular mixture being used for simulation. In case of a binary system, as used in the present work, the hopper space is divided into two layers. The center positions of the bigger particles are generated in the bottom layer and those of the smaller particles in the upper layer. Once the positions of the particles are defined, the function **findrad** is called which finds an allowable radius for each particle. This function gives an allowable radius equal to a fraction of the distance between two particles. Then the particle radii are adjusted by expanding in such a way that there is no overlapping between particles and that the particle radii are in a close range of the particle radii

inputted earlier as simulation parameter. In the process of expansion of the particles, contact forces are calculated (using Walton-Braun model) between overlapping particle, and the subsequent motions are determined through the equations of motion using functions **integ1** and **integ2**. This radii expansion procedure continues for several cycles till the aforesaid geometric constrains are satisfied.

It may be noted that in the radii expansion process a virtual environment of collision of particles is created, however, there is external disturbance, and therefore, the particles are finally set in static equilibrium. Also, the algorithm actually sets the particle radii in a range similar to the actual size distribution.

2.3 Zones Mapping

As the simulation of a physical system may involve a very large number of particles, efficient management of computation and the available memory is of utmost importance in the development of the computer code. For this purpose, the entire space of the hopper is divided into several computational zones. These zones are first mapped; this is done by the function **zonesmapping** where each zone is given a 'zone index' and also each zone has the details of surrounding zones in an array. This function along with other functions, described in the next section, plays an important role in achieving the objectives of memory management and computation time reduction.

2.4 Zones Updating and Neighbor List

The concept of linked lists in the programming languages provides an efficient way to handle the details of a particle and its neighbor. A linked list is a list of similar items linked to each other in a meaningful way for an easy access. First the particles are placed

in different zones which are indexed using the function **zoneindex**. Once the details of the particles in the different zones are known, the function checks the distance between two particles in a particular zone and its adjacent 26 zones. Avoiding the calculation of the distance between each and every particle of the system of particles results in a considerable saving of computational time. The parameter search radius is used by the function to put the particles within this radius in the linked list. This is done by comparing the search distance with the above computed particle distances. Thus the list is minimized to allowable limit to maximize the simulation speed. They are mentioned in detail in APPENDIX B.

2.5 Force Model

Walton and Braun [19] and Walton [20] have developed two separate models for the calculation of normal and tangential forces between two colliding soft spheres. These models are described briefly in the following.

2.5.1 Normal Force Model

This model for normal force calculations, termed as "partially latching-spring model" by Wanton and Braun [19] is shown in Figure 2.1. The collision between the particles is considered to be in the loading and unloading stages. Compression occurs during loading stage and continues until the relative velocity between the particles is reduced to zero and a maximum value of overlap is reached. This is followed by the unloading stage or restitution stage in which separation occurs between the particles. At the end of this stage,

the two particles will either have regained their original shape or have some residual deformation before loading again. No permanent deformation of the spheres is allowed and if the particle does not suffer another collision during the unloading period, any residual deformation is set to zero for the next collision.

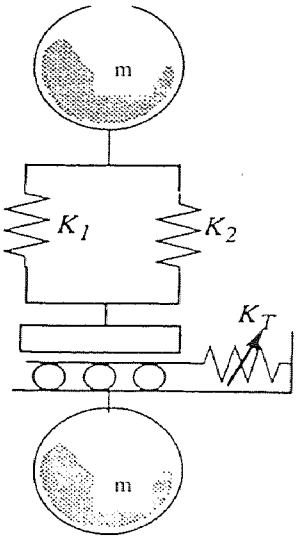

Figure 2.1 Partial latching spring model of Walton and Braun [20]

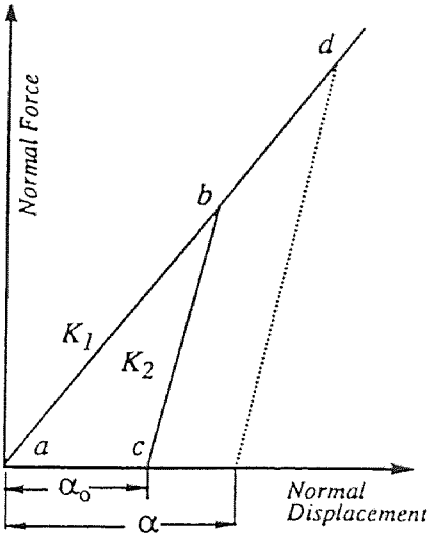

Figure 2.2 Inelastic normal force-deflection curve

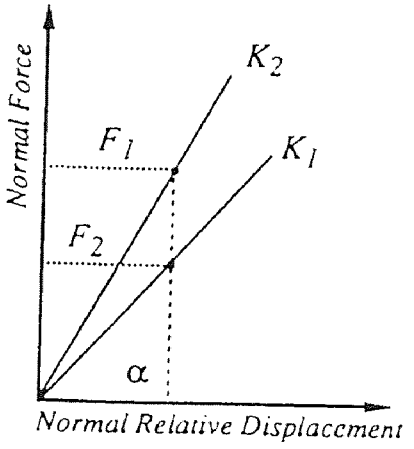

Figure 2.3 Normal force for Case 1

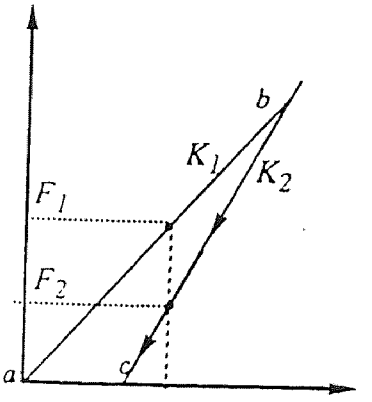

Figure 2.4 Normal force for Case2

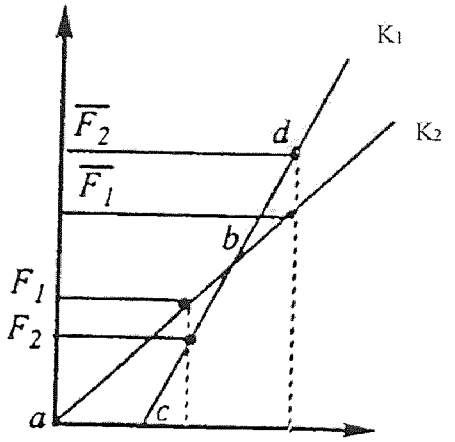

Figure 2.5 Normal force for Case3

As shown in Figure 2.2, the normal force (F_1 or F_2) is expressed as

$$F_N = \begin{cases} F_1 = K_1 \cdot \alpha & \text{For loading} \\ F_2 = K_2 \cdot (\alpha - \alpha_0) & \text{for unloading, or reloading from nonzero overlap,} \end{cases}$$

where K_1 and K_2 are the stiffness of two springs in Figure 2.1, and are the slopes of the loading/unloading lines in the Figure 2.2. Also, α is the instantaneous overlap and α_0 is the overlap value where the loading/unloading curve goes to zero along the slope K_2. In this model, the initial loading follows the slope K_1 from point a to b. If unloading occurs at point b, it will take place along the steeper slope of K_2 from point b to c, until the normal force is reduced to zero with a remaining overlap α_0. Reloading from any point between b and c will follow the path c-b-d. Unloading from a different point d will be along a different path but at the same slope of K_2.

During the simulation, the code calculates the value of F_1 and F_2 at each time step, and chooses the smaller one to be the normal force between the particles, which results in the loading, unloading, and reloading paths as described above. A detailed explanation is as follows.

Case 1:

Loading from zero remaining overlap ($\alpha_0 = 0$), Figure 2.3:

Since $K_1 < K_2$, $F_1 = K_1 \cdot \alpha < K_2 \cdot (\alpha - 0) = F_2$, so that F_1 is the normal force in this case.

This means loading follows the path having a smaller slope K_1.

Case 2:

Unloading:

Unloading from point b will follow the path b-c (Figure 2.4). Here F_2 will always be less than F_1.

Case 3:

Reloading from $\alpha_0 \neq 0$:

From Figure 2.5, it is clear that $F_2 < F_1$ when reloading from c to b. Choosing F_2 as the normal force is equivalent to reloading along path c-b (slope K_2). After reaching point b, F_2 will be larger than F_1. So F_1 will be used as the normal force, ensuring further loading along b to d.

Although the normal force model discussed above is a simple empirical model, Walton and Braun[20] had shown that it could effectively approximate the behavior observed in experiments and finite element calculations. In this study, this model had been used to simulate the behavior of vibrating Hoppers. Results compared with experimental data also demonstrate the effectiveness of this model.

The force model produces binary collisions with a constant coefficient of restitution give by $e = \sqrt{K_1 / K_2}$.

2.5.2 Tangential Force Model

The tangential force model according to Walton [20] is a two-dimensional (surface) extension to Walton and Braun's one-dimension approximation to elastic frictional sphere contact force model of Mindlin [31]. In the tangential force model, the effective tangential stiffness of a contact decreases with tangential displacement until it is zero when full sliding occurs. In the present two-dimensional surface model the tangential displacement parallel to the current friction force and the displacement perpendicular to the existing friction force are considered separately. They are later combined vectorially and their sum is checked against the total friction force limit, μF_N.

The effective tangential stiffness in the direction parallel to the existing friction force is given by:

$$K_T = \begin{cases} K_0\left(1-\dfrac{T-T^*}{\mu F_N+T^*}\right)^{\gamma} & \text{, for T increasing,} \\ K_0\left(1-\dfrac{T^*-T}{\mu F_N+T^*}\right)^{\gamma} & \text{, for T decreasing.} \end{cases}$$

where K_0 is the initial tangential stiffness; T is the current tangential force magnitude; T^* starts as zero and is subsequently set to the value of the total tangential force, T, whenever the magnitude changes from increasing to decreasing, or vice versa; γ is a fixed parameter often set to 1/3 to make the model resemble Mindlin's elastic frictional sphere theory, and μ is the coefficient of friction. A value of 1 or 2 for ν more closely mimics the behavior of frictional contacts involving plastic deformation in the contact region.

This implementation involves some algebraic and vector manipulation since the direction the surface normal at contact changes continuously during a typical contact. The assumption in the model is the time difference between two steps is relatively small. Hence for two spheres in contact if the unit vector normal at the contact point between the two spheres is $\hat{k}_{ij}$. The tangential force in the previous time step is projected on the current tangent plane,

$$T_0 = \hat{k}_{ij} \times T_{old} \times \hat{k}_{ij}$$

$$= T_{old} - \left(\hat{k}_{ij}.T_{old}\right)$$

This projected friction force is normalized to the old magnitude to obtain a new starting value for friction force, before adding in the effects of displacements during the last time step,

$$T = |T_{old} / T_0| T_0$$

A unit vector in the direction of this vector is used in the subsequent steps

$$\hat{t} = T / |T|$$

The relative surface displacement of the last time step projected on to the contact tangent plane is give by,

$$\Delta s^{n-1/2} = \left[\hat{k}_{ij} \times \left(v_j^{n-1/2} - v_i^{m-1/2}\right) \times \hat{k}_{ij} + r_i\left(\bar{\omega}^{n-1/2} \times \hat{k}_{ij}\right)\right]\Delta t$$

$$= \Delta r_{ij} - \hat{k}_{ij}\left(\hat{k}_{ij} . \Delta r_{ij}\right) + \left[r_i\left(\bar{\omega}_i^{n-1/2} \times \hat{k}_{ij}\right) + r_j\left(\bar{\omega}_j^{n-1/2} \times \hat{k}_{ij}\right)\right]\Delta t$$

where $\Delta r_{ij} = r_{ij}^n - r_{ij}^{n-1}$ is the change in the relative position vector during the last time step. For a sphere I and J the subscripts i and j are given, v is the velocity vector ω is the angular velocity and r is the sphere radius and Δt is the time step.

2.6 Boundary Conditions

Boundary conditions need to be applied to check the distance of a particle in the vicintiy of hopper wall. If r_{pw} is the shortest distance between a particle and hopper wall, then overlapping occurs when $r_{pw} \leq r$, where r is the radius of the particle. In Figure 2.6, two

situations, when a particle is close to the vertical side and slant side walls of the hopper, are shown. Particles are initially deposited and then they are vibrated. In the first case of deposition the plane boundary condition is applicable. Where as the case where the hopper vibrates then the walls are not stationary hence plane boundary conditions cannot be applied. The walls of the hopper is allowed to oscillate based on the applied vibration.

Consider Figure 2.6.a The distance r_{pw} is given by

$$r_{pw} = y_{max} - y$$

For the case when the particle is close to the slant side, Figure 2.6.b

$$r_{pw} = [y_{max} - y_1 - (H - z_1) \tan \alpha] \cos \alpha$$

The above equations apply in case of a vibrating hopper as well with z replaced by $z = z + a \sin \omega t$ where a and ω are the amplitude and angular frequency of vibration. t is the time.

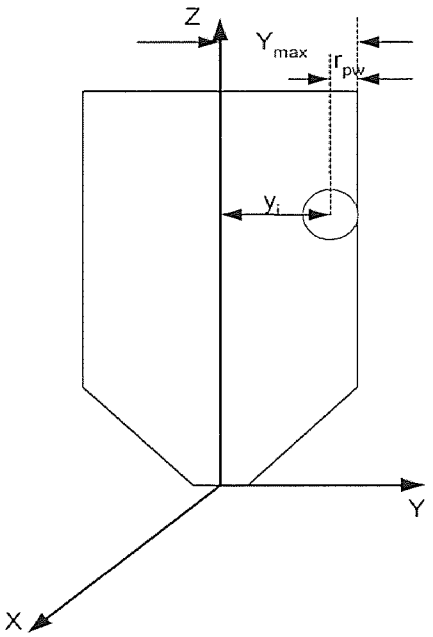

Figure 2.6.a Particle interaction with side wall

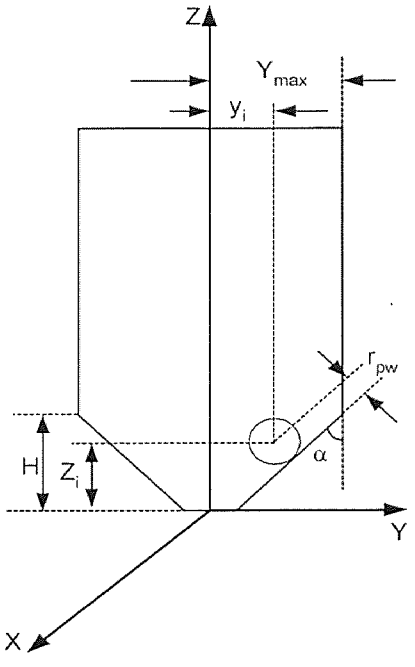

Figure 2.6.b Particle interaction with the slant wall

2.7 Simulations

2.7.1 Simulation of Monodisperse System

A deep bed model of the Hopper similar to experimental system was constructed. In order to study the behavior, a monodisperse system(Figure 2.7) is initially taken and the parameters like frequency and amplitude was varied and studied. The motion of the particle was visually observed using a visualization tool developed in OpenGL. Also the results are plotted in matlab to study the behavior of the particles in the bed. The particle diameter studied was 3.4mm with other parameters of the hopper listed in the APPENDIX C.

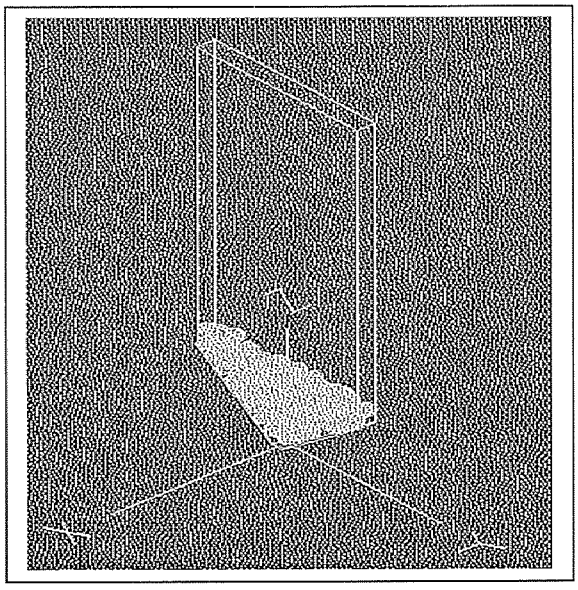

Figure 2.7 Deposited monodisperse system in simulation after 0.5 seconds

2.7.2 Simulation of Binary System

A binary system with two different sized particle was taken for the simulation. To mimic the pouring procedure as in the experiment the larger size particle are randomnly

generated in the bottom half of the hopper and the smaller ones in the top half. The are then allowed to deposit freely under gravity. Then (Figure 2.8)this layer position of the particles is taken as the initial condition and all the simulations are done by varying the frequency and amplitude with the parameters listed in APPENDIX D. The parameters like firction factor of the particle/wall was also studied. Also the angle of hopper is varied to study the behavior of the particles.

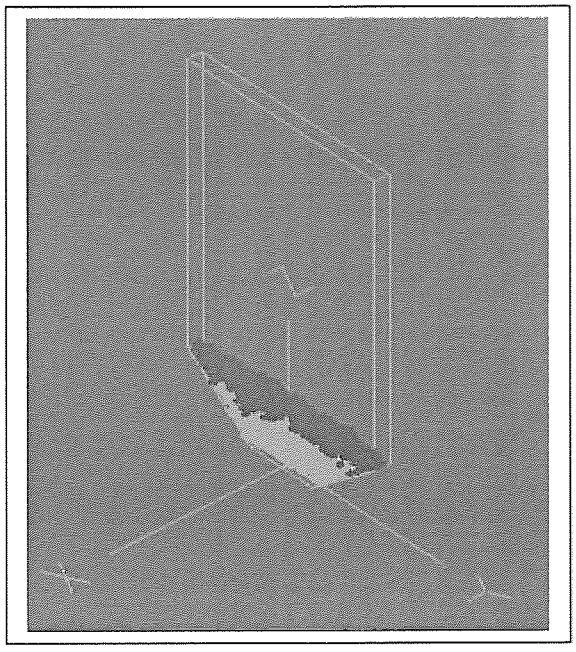

Figure 2.8 Deposited binary system of particles after 0.5 seconds

CHAPTER 3

EXPERIMENTS ON VERTICALLY VIBRATED HOPPERS

Extensive experiments were carried for investigating the granular-flow characteristics in vertically vibrating hoppers. Major facilities for the experiments pre-existed; modifications and additions were made as needed. However, some details of the experimental setup, instrumentation, and experiments are described in the following.

3.1 Experimental Setup

The experimental setup comprised of three components, namely, a hopper, a vibration exciter, and a granules collection system. In the present study, conical or wedge-type hoppers having a passage of rectangular cross-section were used. By taking the thickness of the passage small, the granular motion was essentially confined in one vertical plane, and, therefore, the hoppers may be considered as plane-flow or two-dimensional. This may seen from Figure 3.1, which shows the dimensions of one of the hoppers used; the gross planar dimensions of the hopper are 22 cm height and 15 cm width. With the gross dimensions remaining the same, hoppers with two included angles, namely, 45° and 60°, to simulate the conditions of core flow and mass flow hoppers, respectively, were used for the experiments. The hopper exits were of the size 3mm by 6mm and 14mm by 6mm for the 45° and 60° hoppers, respectively.

The hoppers were made with glass on the front, acrylic on the two sides, and aluminum on the back. The glass wall and acrylic sides obviously provide convenience in granular flow visualization. The pre-existing hoppers were made with glass on the back wall as well. However, experiments on those hoppers lacked consistency in that, under

identical conditions, the granular flow pattern was hardly reproducible. This was considered to be due to the generation of electrostatic charges. Having the back wall of aluminum as grounding dissipated the static electricity actually alleviated the problem of non-reproducibility of results.

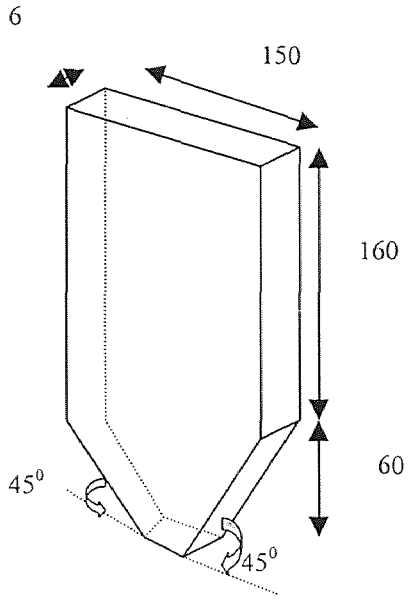

Figure 3.1 Schematic diagram of the 45^0 wedge angle hopper dimensions are in milimeters

In the present study, the hoppers were subjected to vertical vibrations, which were given by mounting the hoppers on a vibration exciter. The photograph of the complete assembly of the experimental setup is shown in Figure 3.2; the exciter shown here is Model V651 Ling Dynamics Vibration Exciter. The mounting of the hopper on the exciter through six studs on the circular plate gives the provision for fixing a hopper at six different angular locations about the vertical axis.

Figure 3.2 also includes the granules collection system. This system has a chain pulled track, operated by an electrical motor. The track can accommodate as many as

twenty-five collection cups. These cups are designed with a parabolic profile at the top to increase the collection efficiency of the granules coming out of the hopper exit. Experiments were conducted for studies on both granular flows inside the hoppers and segregation of binary granules discharging out of the hoppers. In the former case, the hopper opening need to be closed; this was simply done by sticking a thick cardboard piece at the opening.

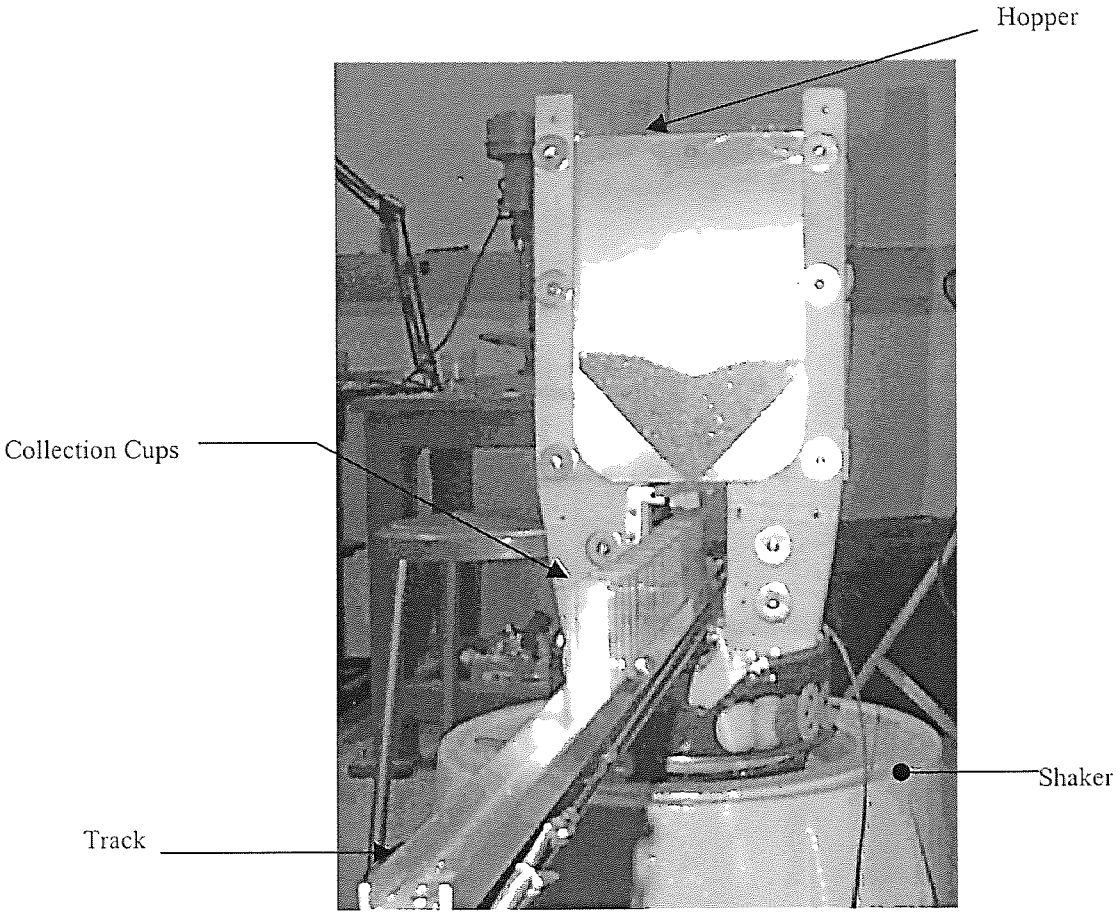

Figure 3.2 Photograph of the experimental setup with the track system

3.2 Instrumentation

The schematic of hopper-exciter assembly and associated instrumentation is shown in Figure 3.3. The vibration exciter is driven through a 1400 VA, Model PA1000L, LDS power amplifier. An accelerometer mounted on the exciter plate to measure the amplitude of acceleration. A digital sign controller (Model DSC 4, LDS) that provides a sinusoidal signal controls the amplifier. This control system can be used for both closed loop and open loop excitations. In a closed loop control, vibration parameters are monitored and corrected automatically through feedback. In this case, excitation builds up gradually to the desired values of vibration frequency and amplitude of acceleration. An open system, which is without feedback, provides excitation close to practical situations as, in this case, vibration builds up immediately. For this reason, the open system was used in the present study. The control system has limit switches to shutdown the system when the frequency or amplitude exceeds the range of the system. Also, the system has a cooling fan, which cools the vibrator from being over heated.

The motor of a CNC milling machine drove the track of the granules collection system; the motor was of course modified for the purpose. A PC operated the track system through the motor, which was loaded with the required CNC program. The track system can be taken to the desired position and also the speed of the track can be controlled.

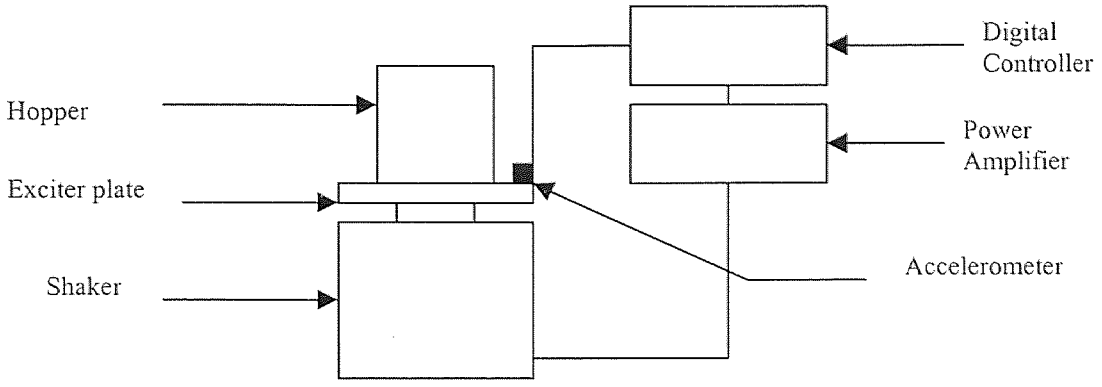

Figure 3.3 Schematic diagram of the experimental setup

3.3 Experiments

The experiments in the present study were carried out basically on binary mixture of granules; experiments with one type of granules were included for the sake of comparisons. Using two types of glass beads of different sizes made the binary mixture. (The details on the specifications of beads will be given in Chapter 4). Also, to felicitate better visualization, smaller glass beads were taken of pink and green color. As will be discussed in Chapter 4, granules in vibrated hoppers exhibit convection pattern. Some experiments included determination of rate of convection. For this purpose one large size, black-dyed bead was placed at the bottom of the hopper, and the time taken by this bead in completing one convection cycle was noted.

In order to have consistency in the initial conditions, the initial setting of the binary mixture of glass modules comprised the layer of smaller sized beads poured over the layer of larger size beads in all the experiments. Experiments were conducted on both

45° and 60° hoppers. In the segregation experiments, the segregation analysis was done by determining the contents of two types of beads in each cup by sieving.

As mentioned earlier, in the present experiments open loop type control was used in vibration excitation. In each experiment, which was done for one set of vibration frequency and acceleration amplitude, care was taken to keep these parameters as close as possible to their pre-set values.

CHAPTER 4

RESULTS AND DISCUSSION

4.1 General

The results of experimental and computer simulation studies on vertically vibrated hoppers are presented in this chapter. The experimental studies include the segregation analysis and flow characterization of binary granular mixtures in wedge-type hoppers. Granular flow patterns were also studied by computer simulation technique and compared with experimental results. As mentioned in chapter 3, two types of planar hoppers of wedge angles 45^0 and 60^0 were used in the present studies. In the experiments four types of spherical acrylic glass beads were used as granules. The specifications of the beads are given in Table 4.1.

Table 4.1 Specifications of the beads used in the experimental studies

Type	Size Range mm	Color	Mass/Density gm/cc	Min% Round
A	4.0-2.8	Colorless	2.5	65
B	1.7-1.4	Green	2.5	80
C	1.0-0.80	Green	2.5	80
D	0.6-0.5	Pink	2.5	80

The binary granular mixtures were made by taking A/D, B / D, and C/D combinations of the beads. The ranges of frequency and acceleration used for present studies were 20-60 Hz and 2-10 g, respectively.

4.2 Experimental Studies

4.2.1 Segregation Experiments

Segregation experiments were done with B/D binary mixtures. In all the experiments all possible care was taken to prepare the binary mixtures in the same manner to ensure as much as possible the uniformity of the mixtures. For each experiment, 50gms of B and D types of beads were taken. The hopper with sealed exit was filled with ten alternate layers of each of the two types of beads, where the bottom layer was of D type beads.

Segregation experiments were done both without and with vibration. Hopper discharge was started by opening the exit. However, in the experiments with vibration, the hopper was allowed to vibrate for 3 minutes before opening the exit. As mentioned in chapter 3 the hopper discharge was collected in cups or cells, and the contents of the D type beads of each cell were determined by sieving. Typical results of selected from the segregation experiments are presented in Figures 4.1 to 4.3. These figures show percent contents of D type beads of each cell. It may be noted that 50% contents of the D type beads imply equal amount of the two types of beads and hence no segregation.

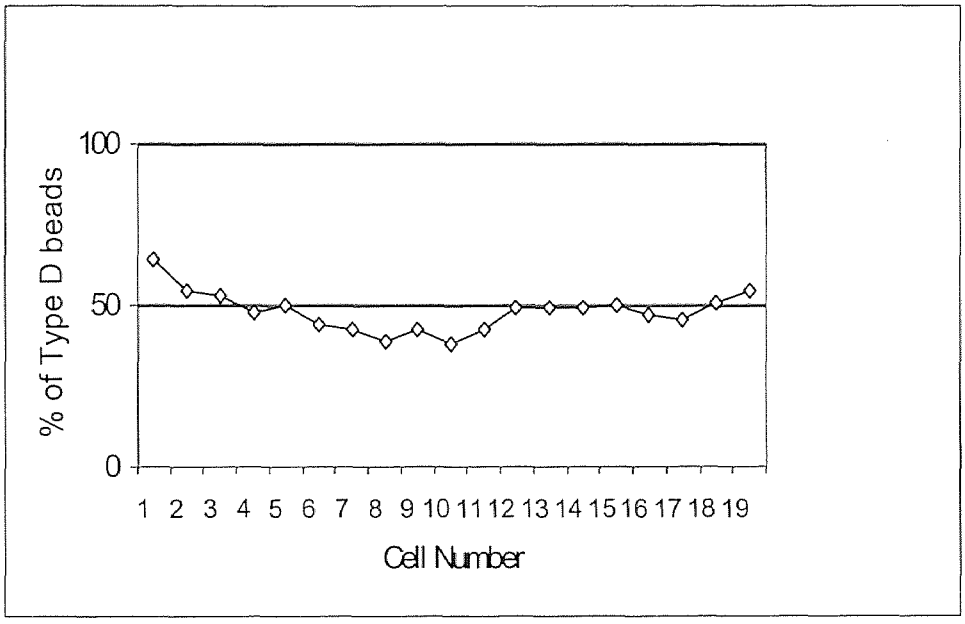

Figure 4.1 Percentage of the D-type beads in various cells discharged from a 45^0-wedge hopper without vibration

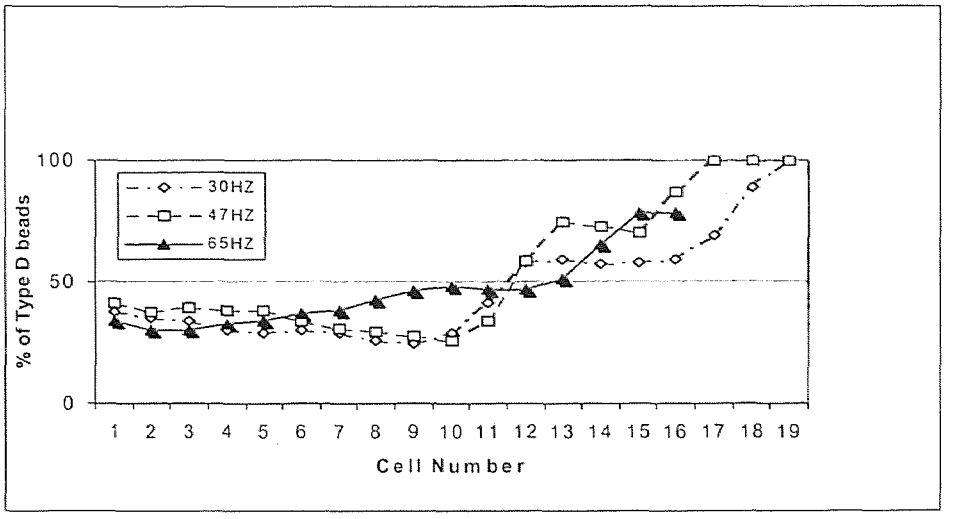

Figure 4.2 Percentage of the D-type beads in various cells discharged from a 45^0-wedge hopper with vibration

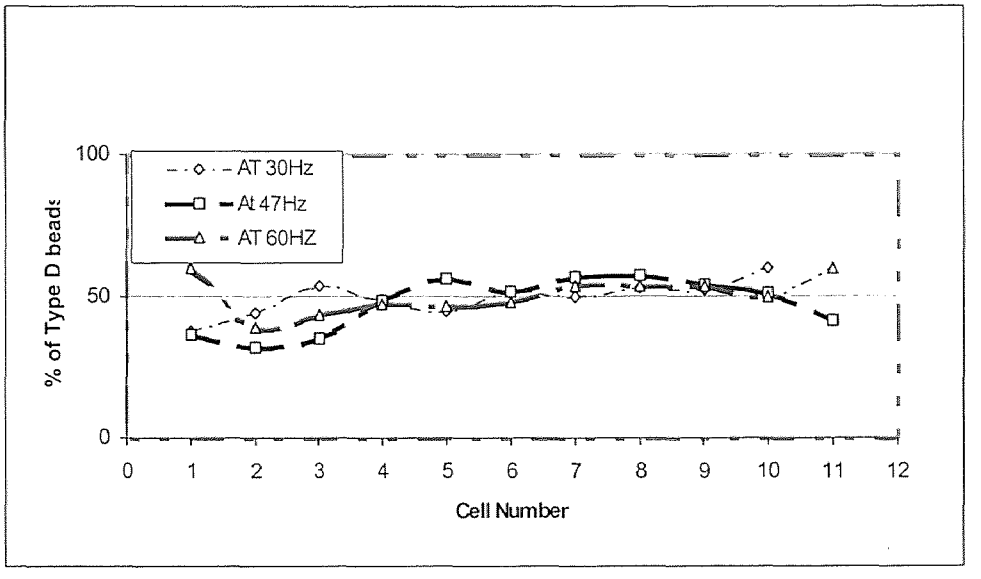

Figure 4.3 Percentage of the D-type beads in various cells discharged from a 60^0-wedge hopper with vibration

The following observations can be made from Figures 4.1 to 4.3

1. As seen from Figure 4.1, initial discharge in the cells from the hopper without vibration has greater contents of the either D or B type of beads. However at the later

stage, the discharge in about one half of the cells is of nearly equal proportions of the two types of beads.

2. The effect of vibration on segregation depends on the wedge angle. As seen from Figure 4.2, the discharge from the 45^0- wedge hopper contains greater proportions of B-type beads in the initial stages and of D-type beads in the later stages. However except for the end cells the discharge from the 60^0 –wedge hopper are more uniform with almost equal contents of the two types of beads.
3. The frequency of vibration does not appear to affect the segregation significantly. However it seems that increase in frequency tends to make the contents of segregated discharge more uniform.

4.2.2 Flow Characterization

Experiments for studying flow characteristics of binary mixtures in vertically vibrated hoppers with closed exits were carried in two parts. The first part of studies were carried out specifically to observe the formation of convection pattern with increasing depth of the binary mixture in the second part, the effects of frequency and acceleration on the flow patterns for binary mixtures beds of fixed depths were studied. The details of these experimental studies are described in the following.

4.2.2.1 Convection Phenomena in Wedge-type Hoppers with Increasing Depth of Binary Mixtures: In these experiments the binary mixture beds was made by layering alternately 5gm each of B (fine) and D (coarse) beads, where the bottom layer was of the coarse beads. In the initial setting, the hopper was filled up to the tapered part and then the depth was increased gradually flow pattern was observed by vibrating the hopper for

various depths of the binary mixture. It may be pointed out that in these experiments the binary mixture beds were always deep in the sense of conventional terminology.

The vibratory experiments with increasing depth of the binary mixture were carried at a fixed g-level acceleration of $\Gamma = 5$ but with the frequency in a range of 20 to 40 Hz. In all these experiments, two types of convection patterns sketched in Figures 4.4 to 4.6 were observed. The important features of the observations are as follows:

1. The flow pattern of the binary mixture, having depth up to the tapered portion of the hopper, is comprised of two distinct convection loops; see Figure 4.4. In each loop, the circulation is such that the beads roll up along the slanted wall. This type of convection loops in vibrated containers with slanted have been reported in some recent works only [15, 25, 26, 32].
2. When the depth of bed is increased such that it covers some part of the vertical sides of the hopper, the convection pattern does not show any noticeable difference, see Figure 4.5. However, as the depth is increased, the rolling up beads of a convection loop deviate earlier from the vertical wall leaving a larger stagnant portion near the vertical sides.
3. After a certain depth, the rolling-up beads which deviate from the vertical wall tend to circulate towards the vertical side in a secondary loop. This phenomenon is shown in Figure 4.6, and as seen the beads in the secondary loop roll down the vertical sides.

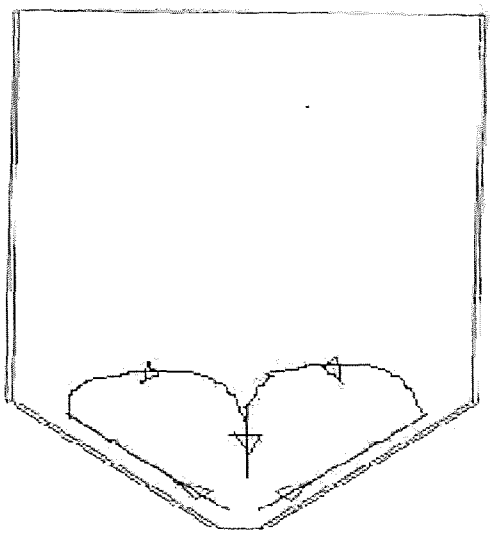

Figure 4.4 Two-loop convection pattern

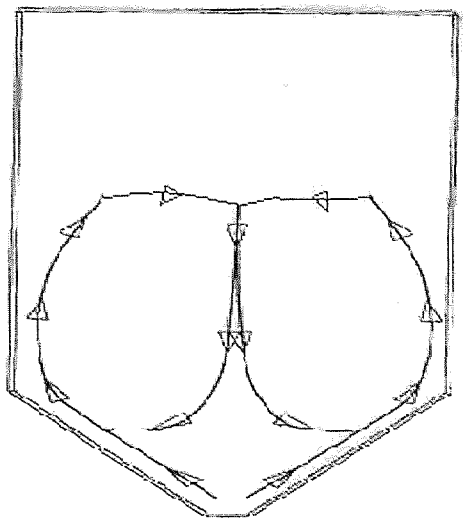

Figure 4.5 Two-loop convection pattern

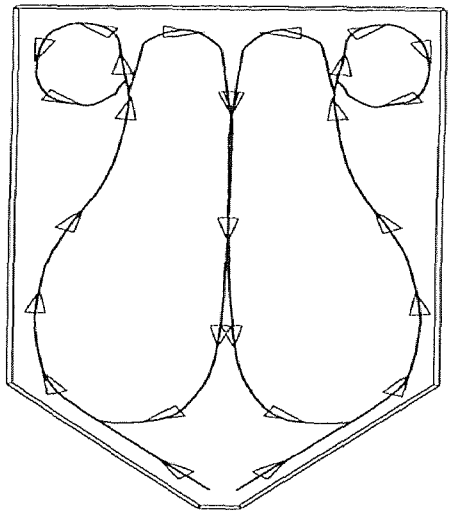

Figure 4.6 Four-loop convection pattern

4. It is shown in several studies that the granules in vertically vibrated rectangular containers roll down the vertical wall [6, 7]. Thus, it is apparent that the convection phenomena observed in Figure 4.6 is in reality a combination of convection phenomena of vertical and slant side containers.
5. The observed convection patterns were independent of the range of frequency considered.

4.2.2.2 Effect of Frequency and Acceleration of Vibration on Flow Pattern of Binary Mixtures in Wedge-type Hopper: Granular beds with two types of binary mixtures were used for these experiments, one with 50 gm each of B and D types of beads and the other with 20 gm each of A and D types of beads. In each case, the bottom layer was of the coarse beads, and the mixtures filled the tapered portion of the hopper. Experiments to observe the granular flows were performed by fixing the frequency or g-level acceleration and varying the other, i.e., g-level acceleration or frequency, in a certain range. The ranges of two vibration parameters were taken as 5 Hz to 50 Hz for the frequency and 2g to 7g for acceleration. The observed pattern for the B and D mixture of granular material are shown in Figures 4.7-4.10.

1. At low acceleration amplitude a two-cell convection patterns begins to form only at the top while the rest of the bed remained unaffected.
2. The convection cells comprised of the fine beads surrounded by circulating coarse beads where, as described earlier the coarse beads were found to roll up the side walls of the hopper.
3. The convection phenomena with the two types of mixtures were basically of the same patterns. However, the accumulation of the smaller D-type beads at the center of the cell was found to be more in case of the larger size ratio A/D mixture than that in the smaller size ratio B/D mixture.
4. The rate of convection increased with increase in acceleration, but decreases with increase in frequency, see Figure 4.11.a.
5. Figures 4.9 shows another type of convection pattern, the so-called 'heaping' or 'bunkering' phenomena, also observed by some authors in vertically vibrated

rectangular containers [6]- [9]. Here, one of the two convection cells dominates, and the top surface becomes inclined at an angle of about 30 degrees from the horizontal. The segregation is still evident in this picture. In the particular case of Figure 4.9, the heap is inclined downward to the right. However, in some other experiments for different combination of frequency and acceleration, heaps sloping down to the left were also observed. At the very glance heaping appears to be occurring due to misalignment. However, this possibility was ruled out since the sloping direction of a heap in particular experiment never changed by flipping the hopper. Recently, some authors have offered explanations for this peculiar phenomenon, however it still remains somewhat obscure.

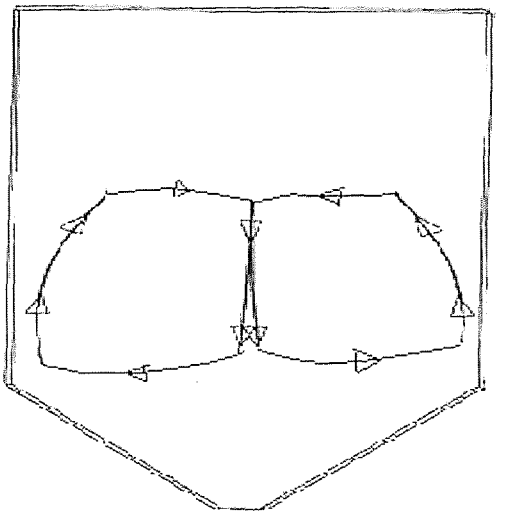

Figure 4.7 Convection pattern at a low amplitude of vibration

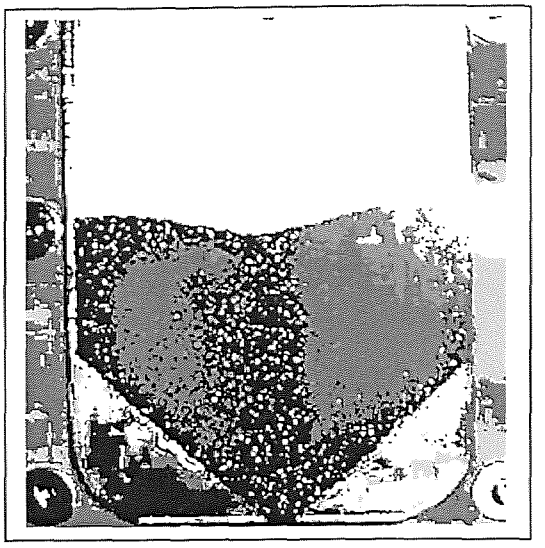

Figure 4.8 Convection cell at 30 Hz frequency and 5 g acceleration for B/D binary mixture

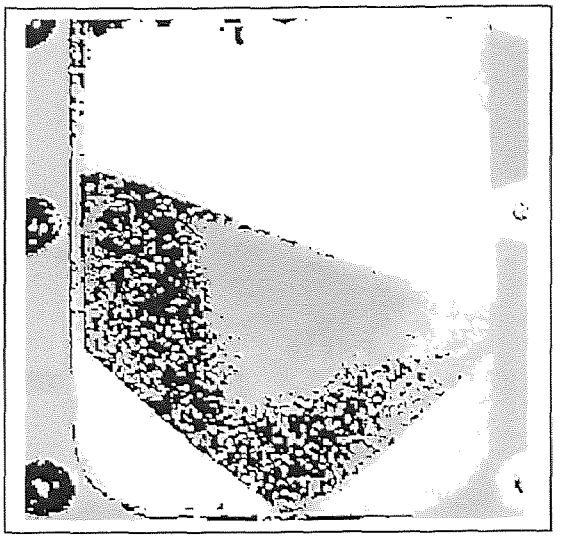

Figure 4.9 Convection cell at 47 Hz frequency and 5 g acceleration for B/D binary mixture

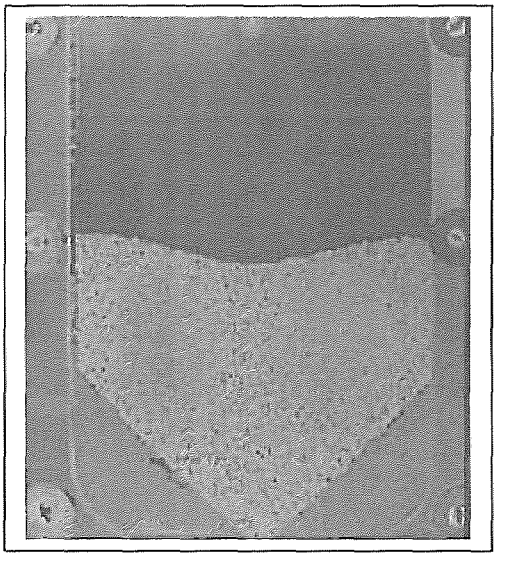

Figure 4.10 Convection cell at 60 Hz frequency and 5 g acceleration for B/D binary mixture

The experimental results of the A and D granular mixture were plotted as follows

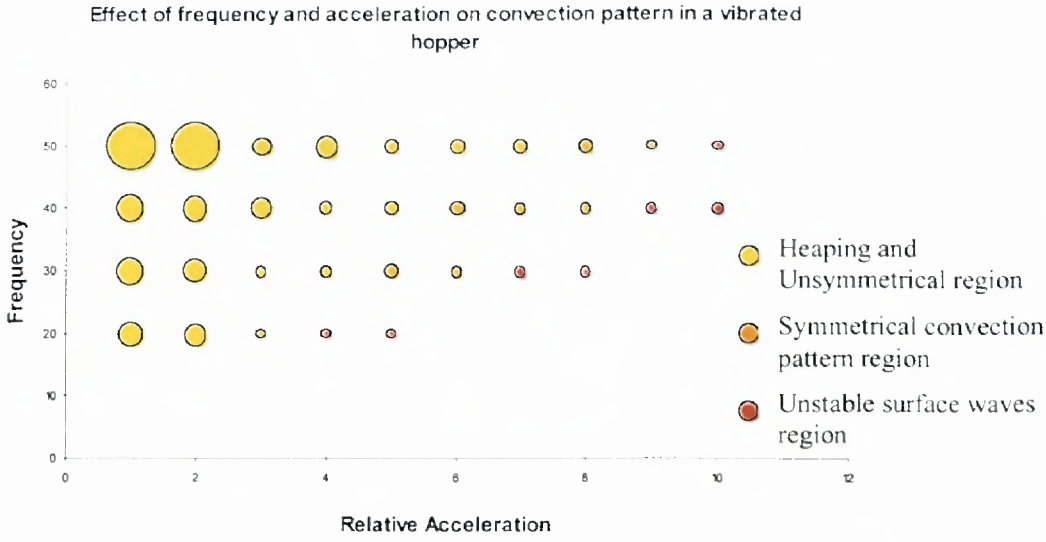

Figure 4.11.a Plot showing the state of the vibrating bed for A/D binary mixtures, at various frequency and acceleration

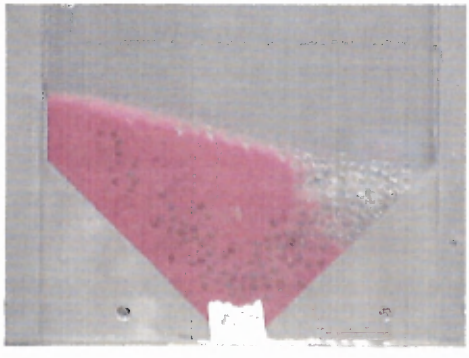

Figure 4.11.b Convection cell for A/D binary mixtures, symmetric at 30 Hz frequency and 3 g acceleration

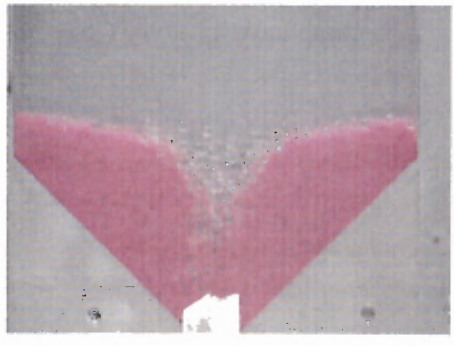

Figure 4.11.c Convection cell for A/D binary mixtures, symmetric at 30 Hz frequency and 5 g acceleration

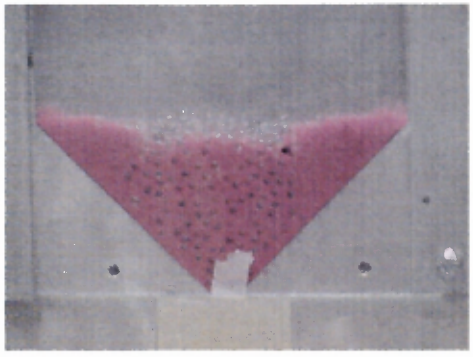

Figure 4.11.d Convection cell for A/D binary mixtures, symmetric at 50 Hz frequency and 10 g acceleration

6. From the space plot Figure 4.11.a for A/D binary mixtures, the granular flow behavior three states of the vibrated bed can observed

- Heaping and unsymmetrical region
- Symmetrical convection pattern region
- Unstable surface waves region

In the first region, it was observed that at low amplitudes at a fixed frequency the movement of the particles in the bed was very slow(Figure 4.11.b). In addition to this, the particles seemed to roll down on the inclined top surface of the bed before reentering the bed. In this region the convection patterns were always unsymmetrical, the yellow bubble in the plot shows this region. The size of the bubble shows the rate of convection of the bubble, bigger the bubble lesser the rate of convection. More experiments should be done to further classify this region.

In the second region, the convection patterns form two loops. The orange bubbles in the plot show this. The size of the bubble decreases which indicates an increase in the rate of convection.(Figure 4.11.c).

The third region observed at higher acceleration amplitude, seem to indicate some instability in the movement of the particles within the bed. For this range there is one complete loop in some cases where as in other cases there is a complete convection pattern with many of surface waves(Figure 4.11.d).

6. Convection patterns seems to form wider bands at lower Amplitude and more streamlined bands at the higher amplitudes for a given frequency.

4.3 Simulation Studies

Simulations of binary mixture flows were carried out in vertically vibrated hopper models. As explained in CHAPTER 2, initial bed setting was done by setting randomly distributed particles under gravity. A mono-disperse system of 3.4mm diameter spherical particles and binary system of 3.4mm diameter spherical particles and binary system of 3.4mm and 1.7mm diameter particles were considered for simulation. The ranges of frequency and acceleration were taken as 20 Hz to 60 Hz and 1 g to 10 g, respectively. The parameters used in the simulation are give in APPENDIX D. The output was printed after twenty cycles of oscillations from where the average displacement vectors of the particles were plotted using Matlab. The convection patterns were also observed using the code developed in Opengl on the SGI machines.

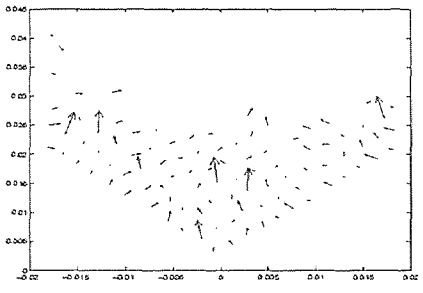

Figure 4.12.a Displacement vectors of the mono-disperse particles after 20 oscillating cycles at frequency of 10Hz and 5 g acceleration

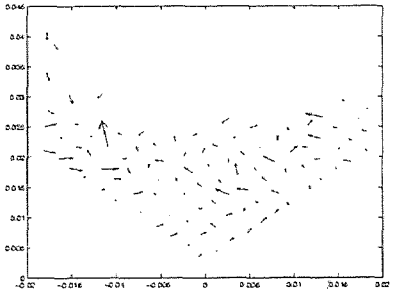

Figure 4.12.b Displacement vectors of the disperse particles after 20 oscillating cycles at frequency of 20Hz and 5 g acceleration

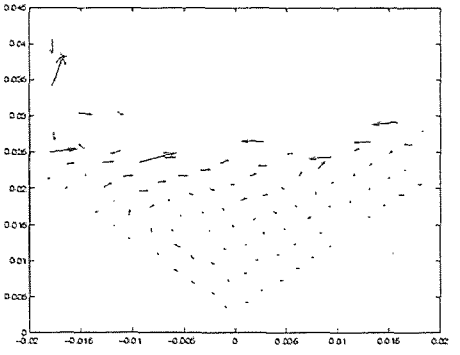

Figure 4.12.c Displacement vectors of the mono-disperse particles after 20 oscillating cycles at frequency of 30Hz and 5 g acceleration

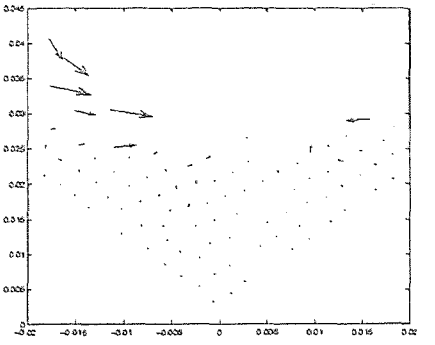

Figure 4.12.d Displacement vectors of the mono-disperse particles after 20 oscillating cycles at frequency of 40Hz and 5 g acceleration

Sample plots of the flow patterns are shown in Figures 4.12.a-4.12.d for the mono-disperse system and in Figures 4.13.a- 4.13.d for the binary system. A discussion on these results follows:

1. It was found that in the very initial stage, the depth of the bed is reduced due to compaction.
2. In the Figure 4.12.d, there are two convection cells, and in each cell, the particles are seen to be rolling up side walls of the hopper and down along the center. Figure 4.12.a shows random motion of the particles which is generally seen when vibrated with very high amplitude.

3. It is also observed from Figures 4.12.a – 4.12.e that the rate of convection increases with increase in acceleration at a fixed frequency, and decreases with increase in frequency at constant acceleration this is indicated by the size of the displacement vectors.
4. In case of the binary system, two-loop convection patterns were observed with the larger beads moving upward along the side walls of the hopper before reentering the bed.
5. Simulation results highlighted by vector plots (Figure 4.13.a-b) also show the symmetrical convection region. Greater detail of particles motion is shown by trajectory plots in Figure 4.13.c , where the path of ten particles were traced and the motion was observed . The path of the particles clearly shows the convection motion within the bed. The particle near the hopper wall moves up along the wall and joins the convection, this motion is shown by the cyan color particle trajectory near the hopper wall.

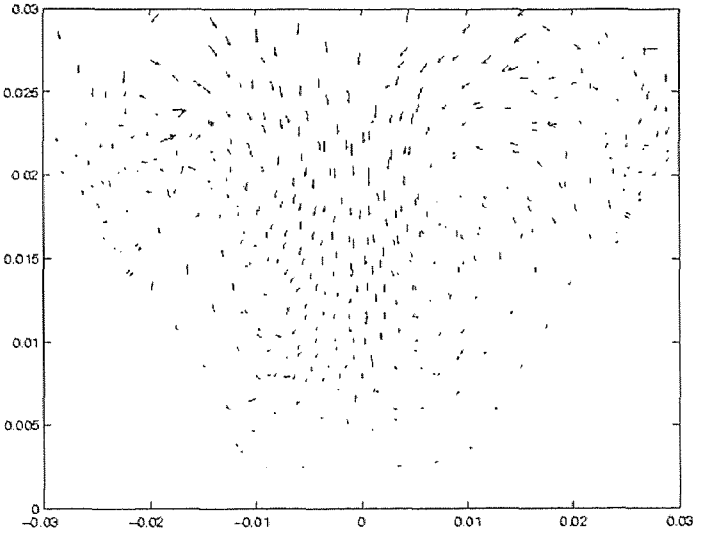

Figure 4.13.a Displacement vectors of the particles for 20 cycles after hundred oscillation cycles at a frequency of 40Hz and 6g acceleration

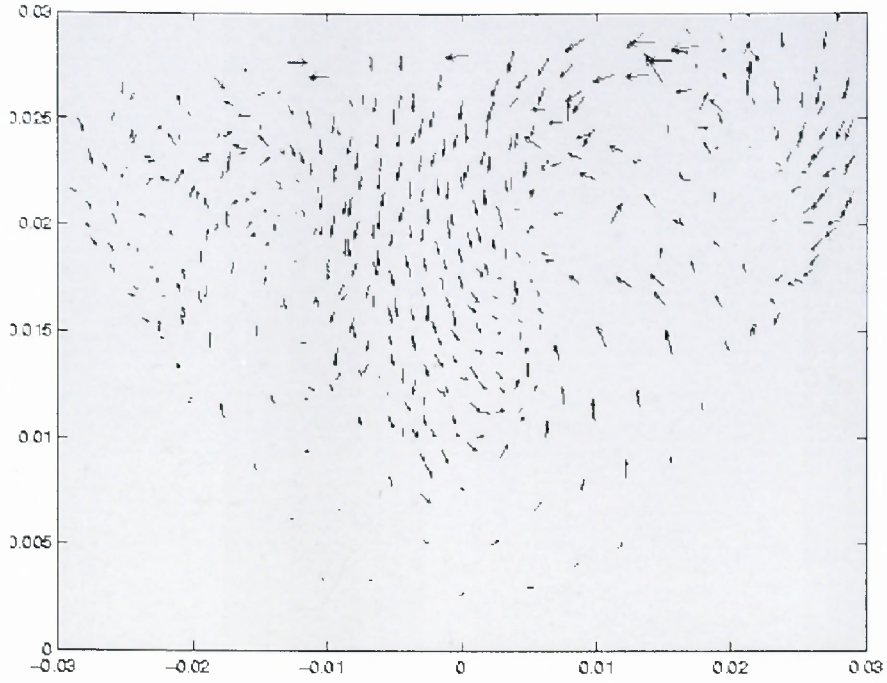

Figure 4.13.b Displacement vectors of the particles for 20 cycles after hundred oscillation cycles at a frequency of 30Hz and 4g acceleration

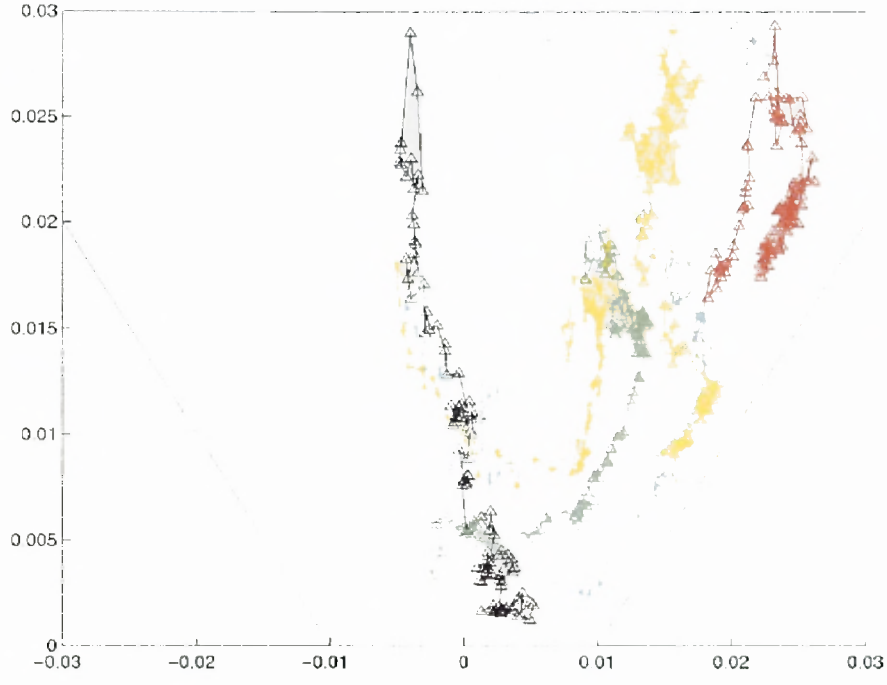

Figure 4.13.c Trajectory of the particles for hundred oscillation cycles at a frequency of 30Hz and 4g acceleration

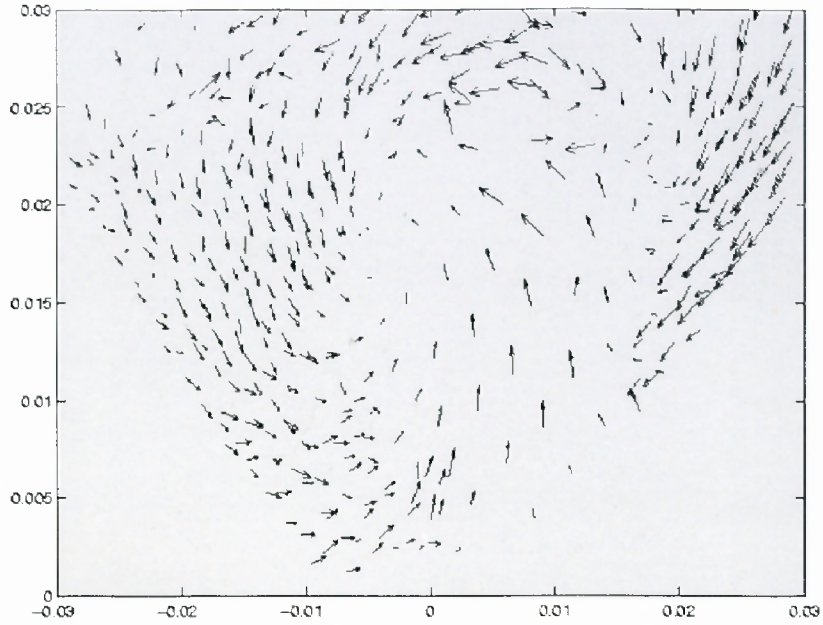

Figure 4.13.d Displacement vectors of the particles for 20 cycles after hundred oscillation cycles at a frequency of 30Hz and 8g acceleration

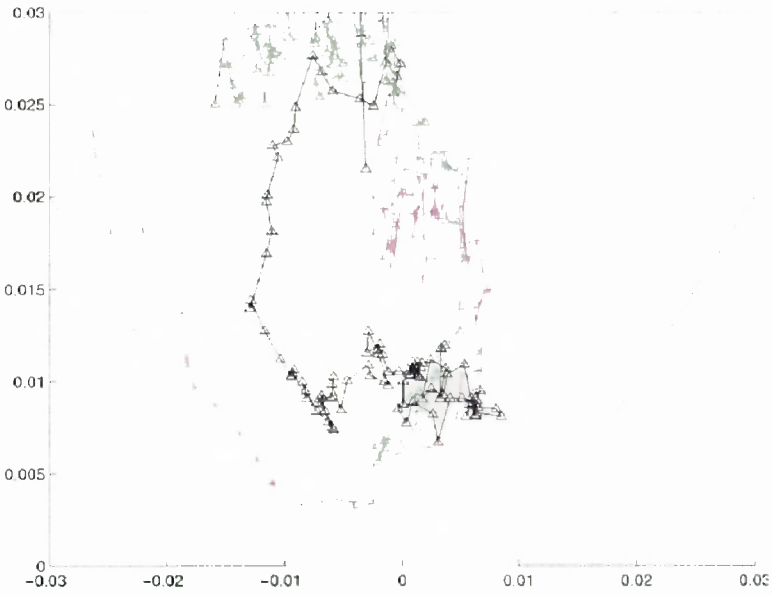

Figure 4.13.e Trajectory of the particles for hundred oscillation cycles at a frequency of 30Hz and 8g acceleration

6. The unstable surface wave region is shown by the vector plot (Figure 4.13.d), where the plot shows a chaotic random motion of the particles. When the trajectory plot Figure 4.13.e is analyzed the pink and black trajectory shows a single convection loop. The particle represented by the green trajectory after reaching the top surface jumps up and down on the surface indicating the presence of surface waves.
7. Though we observe a close qualitative agreement between simulations and experiments in two of the three regions that experimental results show, further simulations should be carried out to validate the experimental results

Although the simulation results generally matched some of the experimental observations, the phenomena of four-loop convection and heaping behavior could not be simulated. It should be noted that because of computational limitations, simulation was done with a very limited number of particles which fills only the conical part of the hopper. This seems to be an obvious reason for not obtaining the four-loop convection pattern by simulation.

To deduce the reasons for heaping, some simulation studies were conducted by changing the parameters of hopper. First, to verify that heaping is not a misalignment-related phenomena, simulation was done by keeping one side wall fixed at 45^0 and varying the inclination of the other side from 40 to 45^0. A tilted top surface, somewhat similar to a heap, was observed initially (shown in Figure 4.14), but it disappeared as the time of simulation was increased. Simulation was also done by changing particle/wall friction. Simulation results with coefficient of friction 0.3 for the front and back walls and 1 for the side wall is shown in Figure 4.15 showed an initial tilt, which, however, disappeared with time.

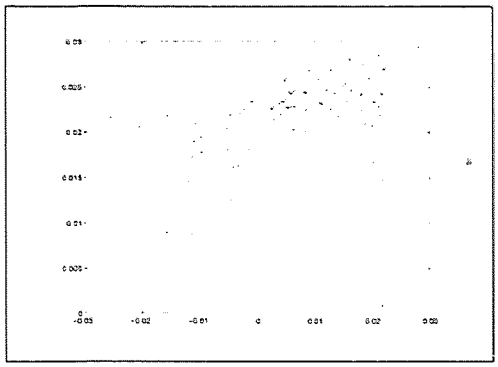

Figure 4.14 Tilt of the top surface due to difference in the hopper angles

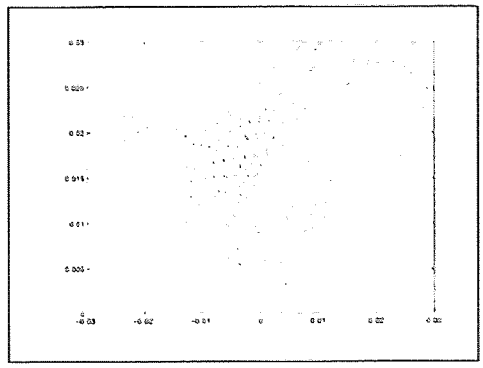

Figure 4.15 Tilt of the top surface due to difference in the wall friction of front and back surface from the side walls

These results indicates that heaping of the vibrated bed may be dependent on the frequency, acceleration amplitude and not due to discrepancy in the hopper geometry or due to the effect of wall friction. Simulations should be carried out for a longer time to explore this state of vibrated bed.

CHAPTER 5

CLOSURE

Research on granular beds in vibrated containers is of continuing interest. This is particularly due to the very practical importance of the problem in wide-ranging industries. Available experimental works have focussed on both segregation and flow characterization. In recent years, numerical simulation has emerged as a powerful tool, which could be used to investigate granular flows with details that may be beyond the physical limits of experiments. A number of simulation studies on mono-disperse beds in vibrated rectangular or V-type planar containers are available in the literature. The research in this thesis also focuses on experimental and simulation studies on vibrated hoppers; however, the work was done with ideas, which are believably not considered in earlier studies. In this work, hoppers of wedge-type with granular beds of binary mixtures were considered. The segregation analysis was done on the basis of the contents of the individual type of granules discharging out of the hopper rather than the time taken by a single large particle from the bottom to the top surface of the bed of finer particles.

The results of the present research may be summarized as under:

1. The results of the segregation study show that vibration promotes segregation of the constituents of binary mixtures. However, increase in frequency was found to make the contents of segregated discharge more uniform. Also, based on the comparison of discharge contents from 45° and 60° wedge angle hoppers, it is found that increase in wedge angle helps in reducing segregation.

2. The experimentally observed flow patterns, such as two-loop convection and heaping were similar to those reported in studies on vibrated rectangular and V-shaped containers.

3. In the convection loops, the granules rolled upward along the inclined and part of vertical sidewalls of the hoppers.

4. Heaping was marked by the shape of the bed with the top surface sloping down from one sidewall to the other. Heaping was accompanied with single convection loop, having the granules moving upward along the sidewall.

5. A new type of four-loop convection pattern, occurring when the bed was deep enough to cover the rectangular part of the hopper, was observed. In this case, from each of the original convection loops grew another small loop near the top surface of the bed. In the smaller loops, the granules moved downward along the vertical sidewalls. The four-loop convection seems to be a combination of the well-reported convection phenomena in V-shape and rectangular containers, and, therefore, is peculiar to wedge-type hoppers.

6. Due to very limited number of particles used in simulation, not all the experimentally observed phenomena could be obtained by simulation. However, generally speaking, simulation revealed some of the experimental observations. Thus, the experimentally observed results for the mixtures shows three regimes, namely, an unstable heaping state, symmetrical convection pattern, and unstable region with surface waves. Convection patterns seems to form wider bands at low accelerations and more streamlined bands at the higher accelerations.

7. No plausible explanation could be found for heaping phenomena.

The present studies bring out many issues, which could possibly be researched in some future studies. These are as follows.

1. The glass beads used in the present experiments were essentially non-cohesive granules. However, granular mixtures in industrial applications are usually cohesive

and semi-cohesive powders, and vibrations are typically used to regulate the mixture-flow through hoppers. Thus, there is an obvious need for segregation studies with the type of granular mixtures as encountered in practice.

2. More experiments must be done with various size ratios of glass beads to clearly characterize the regions seen using the mixture.
3. Simulation studies were severely restrained by the computation time, which grows with the number of particles and decreases with size of the particle.
4. Simulation for cohesive and semi-cohesive particulate beds would further need modification in the code, which presently accounts for the gravitational and contact forces alone.
5. Further experimental and simulation studies are needed on the effect of wedge angle, which is an important parameter.
6. Some recent studies attribute heaping to the presence of horizontal vibrations. Both experimental and simulation studies need consideration of this aspect.

APPENDIX A

FLOW CHART

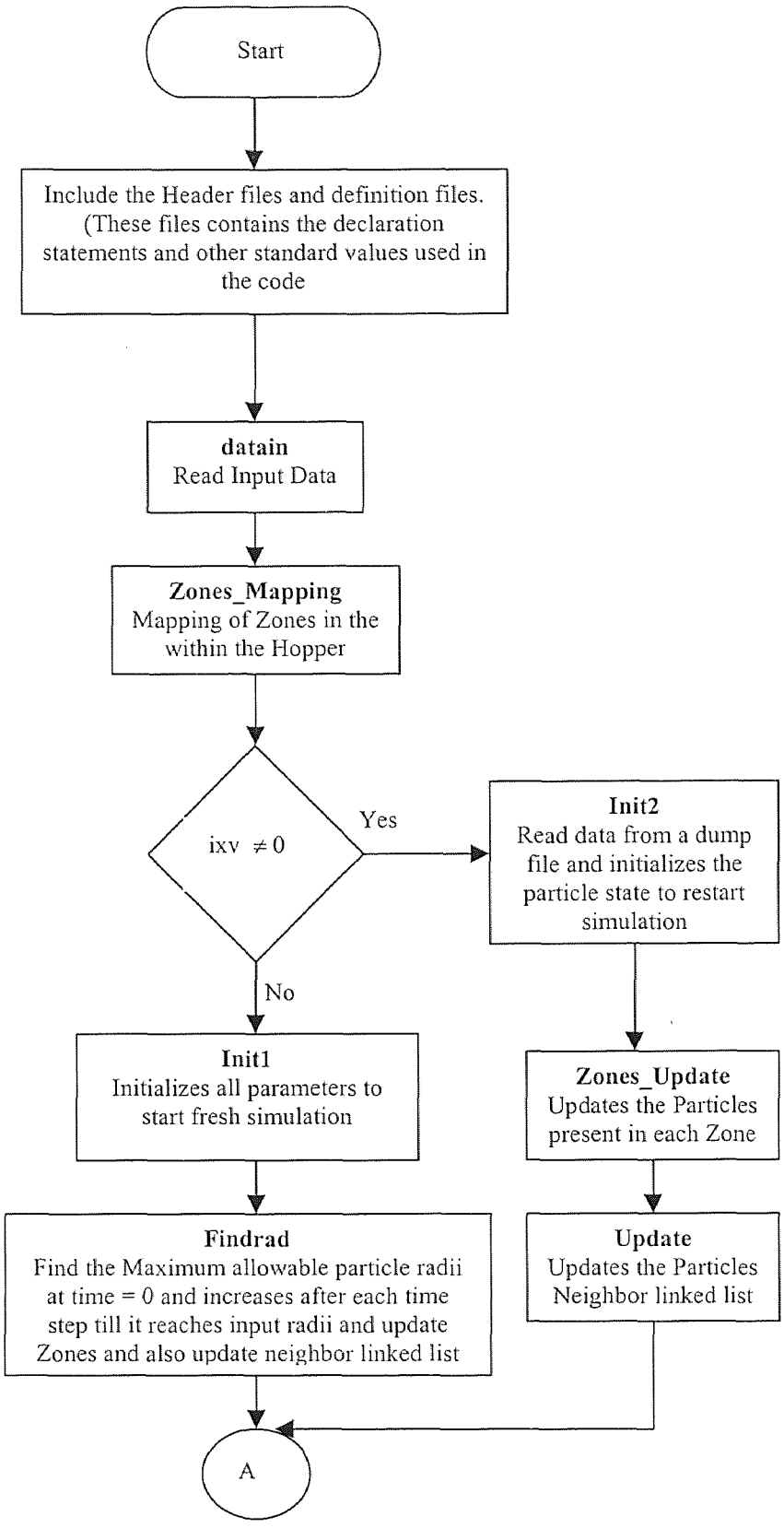

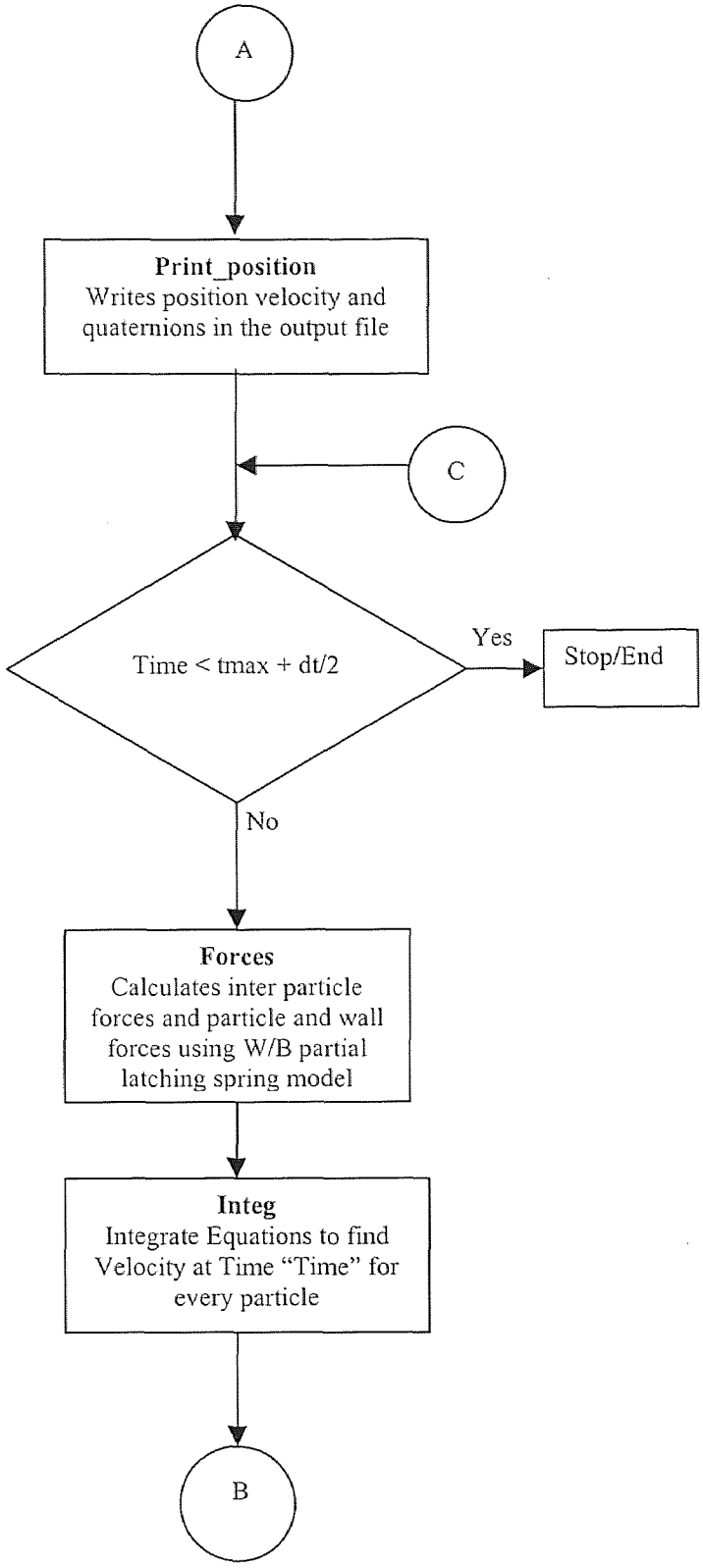
A
Print_position
Writes position velocity and quaternions in the output file
C
Time < tmax + dt/2
Yes
Stop/End
No
Forces
Calculates inter particle forces and particle and wall forces using W/B partial latching spring model
Integ
Integrate Equations to find Velocity at Time "Time" for every particle
B

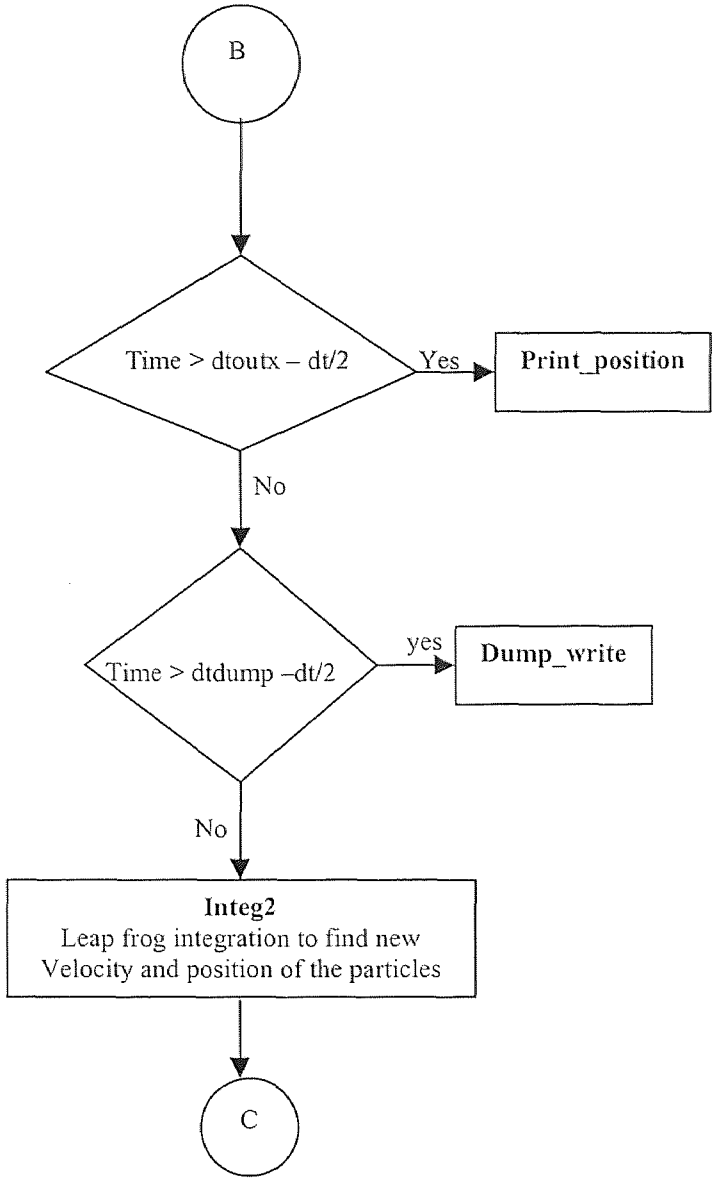
B
Time > dtoutx – dt/2
Yes
Print_position
No
Time > dtdump –dt/2
yes
Dump_write
No
Integ2
Leap frog integration to find new
Velocity and position of the particles
C

Flow Chart of Findrad Function

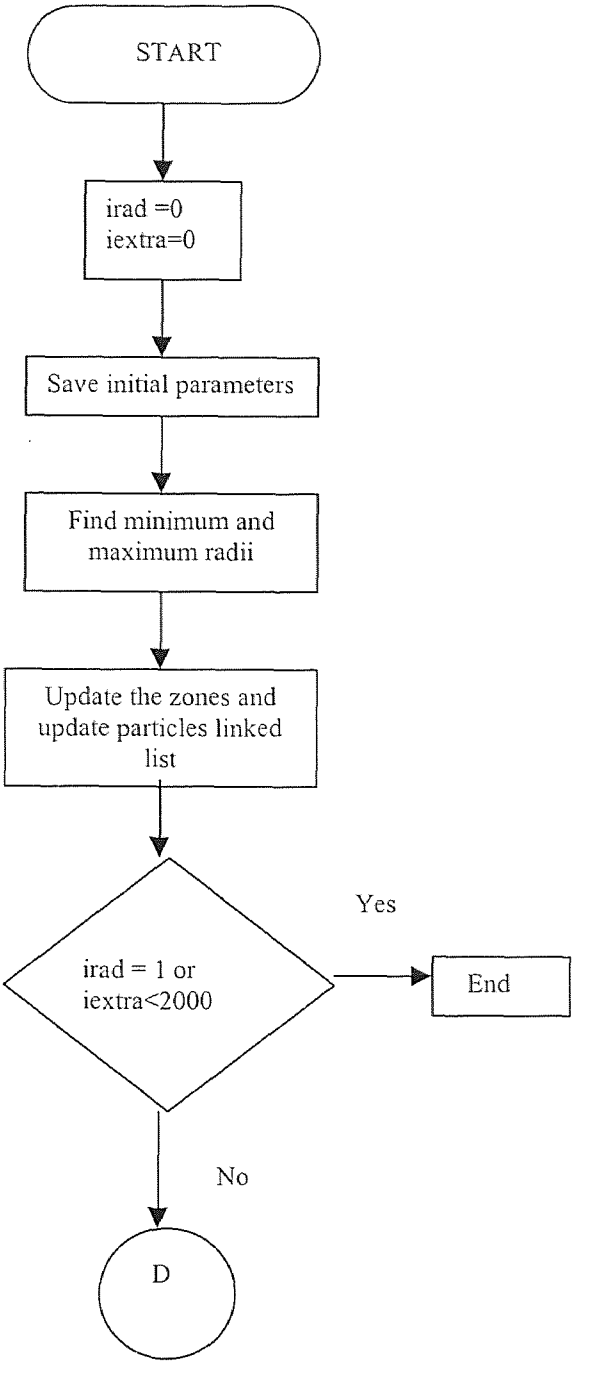

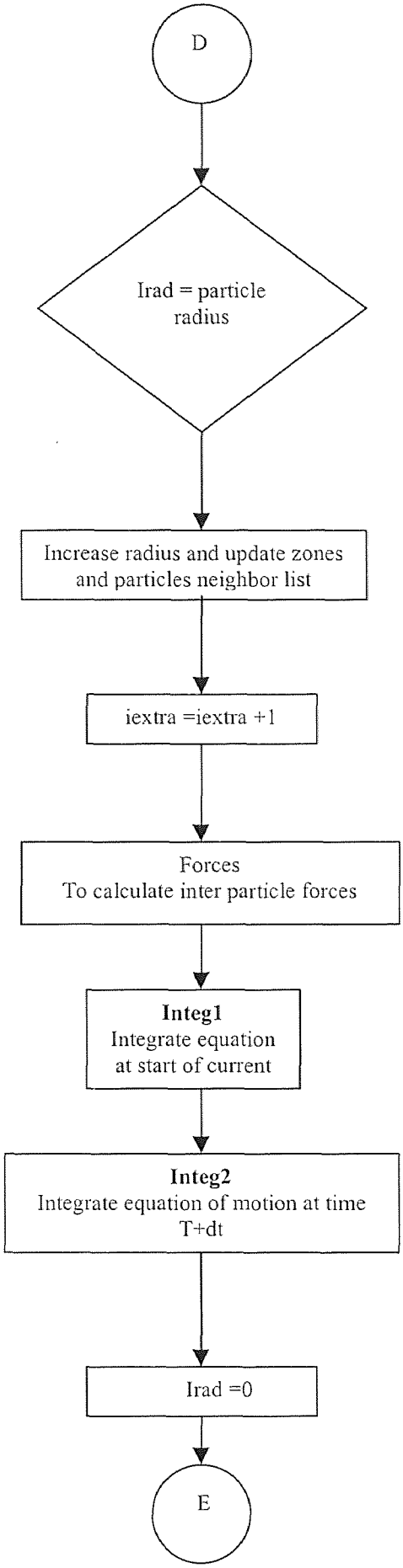
D
Irad = particle radius
Increase radius and update zones and particles neighbor list
iextra =iextra +1
Forces
To calculate inter particle forces
Integ1
Integrate equation at start of current
Integ2
Integrate equation of motion at time T+dt
Irad =0
E

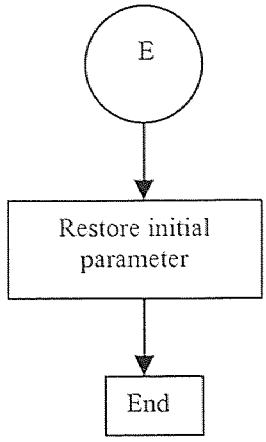
E
Restore initial parameter
End

APPENDIX B

LINK LIST

A list refers to a set of items organized sequentially.

Examples: array, link list.

In an array, the sequential organization is provided implicitly by its index. A completely different way to represent a list is to make each item in the list part of a structure that also contains a "link" to the structure containing the next item.

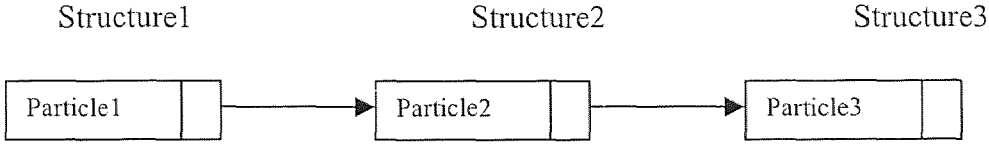

Each structure of the list consists of two fields, one containing the item and the other containing the address of the next item in the list.

Example of a structure

```
Struct particle
{
int particle number;
struct parameters;
struct *particle;
}
```

Advantages of using linked list over an array:

In the case of an array the maximum index should be given while writing the program. Whereas in case of a linked list we can dynamically allocate memory during runtime and thereby we can increase or decrease the list. In the case of simulation the neighbors of a particle and the number of neighbors change during each time interval. So, using a linked

list will be lucrative both in increasing the speed and controlling the memory occupied while running the simulation.

How Link List is used in Maher's Code

Zones Mapping

As the inter-particle force is short ranged the whole simulation volume is divided into 3D cells. Each cell is surrounded by a maximum of 26 cells. Each Zone is given an index number .The function maps the zones around a particular zone including itself.

The mapping reduces the computation time to calculate the distance between the particles residing in the zones other than the mapped zones.

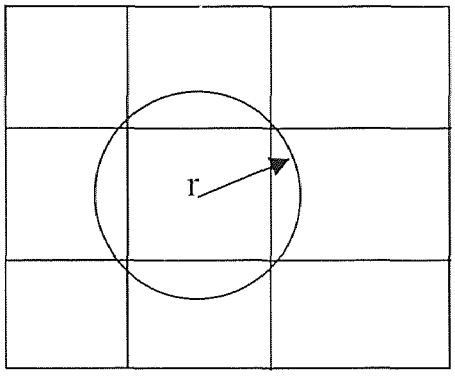

ZonesUpdate

This function finds out the particles existing in each Zone at a particular time.

The Algorithm used here is Hockney-Eastwood .

then the procedure for sorting coordinates into list for each chaining cells by means of address sorting is summarized as follows:

1. Set HOC(q) = -1 for all q.
2. Do for all particles i.

(a) locate cell containing particle

q: = int (x_1 / HC_1, x_2 / HC_2, x_3 / HC_3)

(b) add particle i to head of list for cell q

LL(i): = HOC(q)

HOC(q): = i

This algorithm is explained with an example below

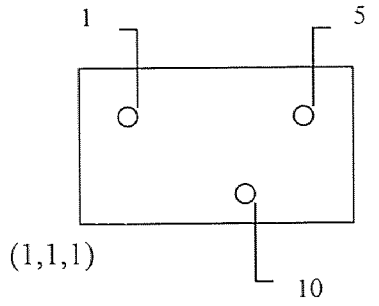

Nx = Number of zones along X axis is 5

Ny = Number of zones along Y axis is 5

Nz = Number of zones along Z axis is 5

i = 1 , j = 1, k = 1

izone = i+j*Nx+k*Nx*Ny

izone = 1+1*5+1*25

= 31

Initially: Zonehead(31) = -1

Loop

- Particle #1

i, j, k = 1, 1, 1

izone = 31

Zone List(1) = zonehead(31) = -1

Zonehead(31) = 1

Where m = 1

- Particle#5

i, j, k = 1, 1, 1

izone = 31

Zone List(5) = zonehead(31) = 1

Zonehead(31) = 5

Where m = 5

- Particle#10

i, j, k = 1, 1, 1

izone = 31

Zone List(10) = zonehead(31) = 5

Zonehead(31) = 10

Where m = 10

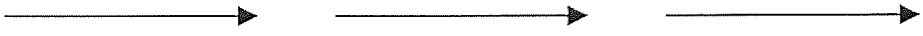

Zonehead(31)=10 ; Zonelist(10)=5 ; Zonelist(5)=1

Update

Now we are having the information of particles present in a particular Cell and also the mapping of Cells around each cell. The flow Chart of program is shown below.

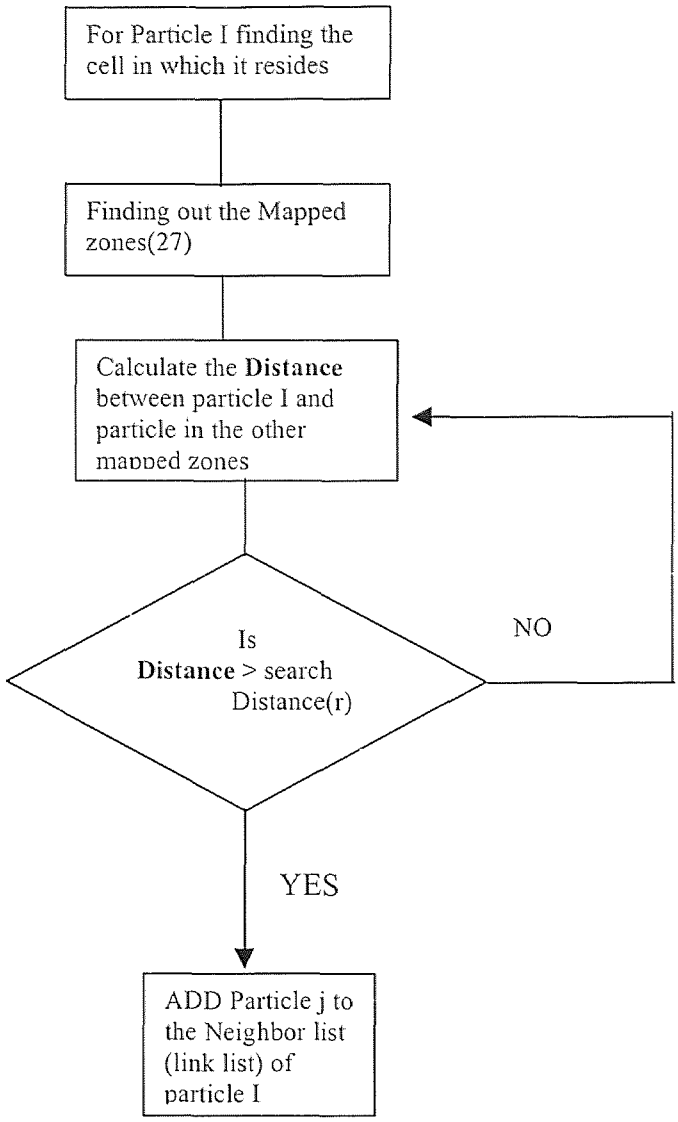
For Particle I finding the cell in which it resides
Finding out the Mapped zones(27)
Calculate the **Distance** between particle I and particle in the other mapped zones
Is **Distance** > search Distance(r)
NO
YES
ADD Particle j to the Neighbor list (link list) of particle I

```
struct neighbor_list_ptr
{
    struct  neighbor_list_ptr *next;
    int  neighbor;
   Contact   part_cont;
}Neighbor_List;

struct part_data_ptr
{
   int nbr;
   Part_Group  *group;
   Int zone;
   Neighbor_List *nlist;
   Int Nnghbr;
   Contact lat_cont;
   Contact side_cont;
   Contact bot_cont;
}Particle;
```

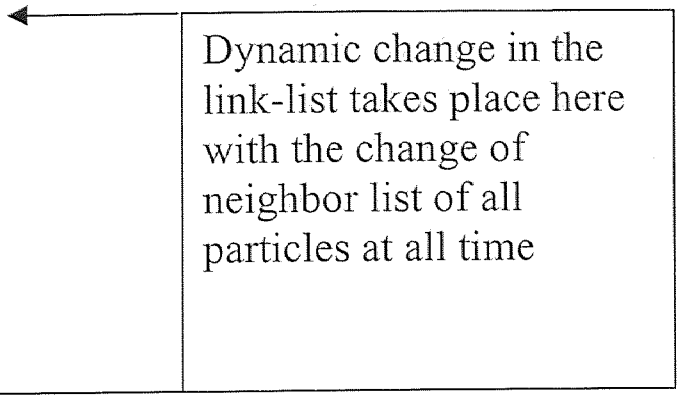

APPENDIX C

SIMULATION PARAMETERS FOR MONODISPERSE SYSTEM

Hopper_Discharge	[Title]
	[Particle data]
1	[GM->Ngroup: Number of groups]
100	[Npart: Group 1 number of particles]
0.0017	[radius: Group 1 particle radius (m)]
5.048e-5	[mass: Group 1 particle mass (Kg)]
1	[GM->Nz[0]: Number of zones in the x-direction]
4	[GM->Nz[1]: Number of zones in the y-direction]
15	[GM->Nz[2]: Number of zones in the z-direction]
	[Boundary data]
0.04	[bndry.L: Boundary width (m)]
0.12	[bndry.H: Boundary height (m)]
0.02	[bndry.D: Boundary distance (m)]
0.0	[bndry.E: Boundary elevation (m)]
0.006	[bndry.W: Boundary thickness (m)]
45.0	[bndry.alpha: Boundary angle (deg.)]
0.0	[bndry.vib1ampl: Amplitude of vibration in the y-direction (m)]
0.0	[bndry.vib1freq: Frequency of vibration in the y-direction (Hz)]
5	[bndry.vib2ampl: Amplitude of vibration in the z-direction (m)]
30.0	[bndry.vib2freq: Frequency of vibration in the z-direction (Hz)]

```
 [ Contact data]
2000.0          [ Kn1:      Normal stiffness coef. (particle-particle) (N/m)      ]
2000.0          [ Kn1b:     Normal stiffness coef. (particle-boundary) (N/m)      ]
0.5             [ rest:     Coefficient of restitution (part-part collision)      ]
0.5             [ restb:    Coefficient of restitution (part-bound collision)     ]
0.7             [ K_ratio:  Ratio of tangential/normal stiffness (particles)      ]
0.7             [ K_ratiob: Ratio of tangential/normal stiffness (boundary)       ]
0.3             [ power:    Tangential force exponent (particles)                 ]
0.3             [ powerb:   Tangential force exponent (boundary)                  ]
0.4             [ mu:       Friction coefficient for part-part contacts           ]
0.2             [ mub:      Friction coefficient for boundary-part contacts       ]
                [ Initialization parameters]
0.0             [ Time:     Initial time for the simulation (s)                   ]
0.66666         [ tmax:     Maximum time for calculation (s)                      ]
0.03333         [ dtoutx:   Time interval for printing positions (s)              ]
0.005           [ dtdump:   Time interval for dumping (s)                         ]
30              [ ntcol:    Number of time-steps during a collision               ]
0.03            [ search:   Search distance for near neighbors (m)                 ]
-9.80665        [ grav:     Acceleration of gravity (m/s^2)                       ]
10.0            [ draddt:   Rate of increase of particle radii (m/s)              ]
0.02            [ vave:     Initial average velocity (m/s)                        ]
0.0             [ V0:       Initial average velocity in the gravity direction     ]
2               [ ixv:      Flag for reading positions and velocities             ]
```

APPENDIX D

SIMULATION PARAMETERS FOR BINARY SYSTEM

Hopper_Discharge	[Title]
	[Particle data]
2	[GM->Ngroup: Number of groups]
50	[Npart: Group 1 number of particles]
0.0017	[radius: Group 1 particle radius (m)]
5.048e-5	[mass: Group 1 particle mass (Kg)]
450	[Npart: Group 2 number of particles]
0.00085	[radius: Group 2 particle radius (m)]
5.048e-6	[mass: Group 2 particle mass (Kg)]
1	[GM->Nz[0]: Number of zones in the x-direction]
4	[GM->Nz[1]: Number of zones in the y-direction]
15	[GM->Nz[2]: Number of zones in the z-direction]
	[Boundary data]
0.04	[bndry.L: Boundary width (m)]
0.12	[bndry.H: Boundary height (m)]
0.02	[bndry.D: Boundary distance (m)]
0.0	[bndry.E: Boundary elevation (m)]
0.006	[bndry.W: Boundary thickness (m)]
45.0	[bndry.alpha: Boundary angle (deg.)]
0.0	[bndry.vib1_ampl: Amplitude of vibration in the y-direction (m)]
0.0	[bndry.vib1_freq: Frequency of vibration in the y-direction (Hz)]

```
5                [ bndry.vib2_ampl: Amplitude of vibration in the z-direction (m) ]
30.0             [ bndry.vib2_freq: Frequency of vibration in the z-direction (Hz) ]
                 [ Contact data]
2000.0           [ Kn1:      Normal stiffness coef. (particle-particle) (N/m)      ]
2000.0           [ Kn1b:     Normal stiffness coef. (particle-boundary) (N/m)      ]
0.5              [ rest:     Coefficient of restitution (part-part collision)      ]
0.5              [ restb:    Coefficient of restitution (part-bound collision)     ]
0.7              [ K_ratio:  Ratio of tangential/normal stiffness (particles)      ]
0.7              [ K_ratiob: Ratio of tangential/normal stiffness (boundary)       ]
0.3              [ power:    Tangential force exponent (particles)                 ]
0.3              [ powerb:   Tangential force exponent (boundary)                  ]
0.4              [ mu:       Friction coefficient for part-part contacts           ]
0.2              [ mub:      Friction coefficient for boundary-part contacts       ]
                 [ Initialization parameters]
0.0              [ Time:     Initial time for the simulation (s)                   ]
0.66666          [ tmax:     Maximum time for calculation (s)                      ]
0.03333          [ dtoutx:   Time interval for printing positions (s)              ]
0.005            [ dtdump:   Time interval for dumping (s)                         ]
30               [ ntcol:    Number of time-steps during a collision               ]
0.03             [ search:   Search distance for near neighbors (m)                 ]
-9.80665         [ grav:     Acceleration of gravity (m/s^2)                       ]
10.0             [ draddt:   Rate of increase of particle radii (m/s)              ]
0.02             [ vave:     Initial average velocity (m/s)                        ]
```

0.0	[V0:	Initial average velocity in the gravity direction	]
2	[ixv:	Flag for reading positions and velocities	]

REFERENCES

1. Chladni, E.F.F.,1787, "Entdeckungen üeber die theorie des klangen," Leipzig, German.

2. Faraday. M.,1831, "On a peculiar class of acoustical figures and on certain forms assumed by groups of particles upon vibrating elastic surfaces," *Phil. Trans. R. Soc. London*, 52:299-340.

3. Bachmann, D., *Verfahrenstechnik Z.V.D.I. Beiheft*, No. 2, pg.43, Düsseldorf, Germany.

4. Kroll, W., 1954, "Fliessersheinungen an haufwerken in schwingenden gefassen" *Chemie Ing. Tech.*, 27:33-38.

5. Thomas, M. O. M., Y. A. Liu, A. M. Squires, 1989, "Identifying states in shallow vibrated beds," *Powder Tech.*, 2:267-280.

6. Wassgren, C. R., C. E. Brennen, M. L. Hunt, 1996, "Vertical vibration of a deep bed of granular material in a container," *J. Appl. Mech*, 63:712-719.

7. Wassgren, C. R., 1997, *Vibration of Granular Materials*, Ph.D. Thesis, Department of Mechanical Engineering, California Institute of Technology, Pasadena, CA.

8. Fauve, S., S. Douady, S., C. Laroche, 1989, "Collective behaviors of granular masses under vertical vibration", *J. Phys. France*, 50:187-191.

9. Evesque, P., J. Rajchenbach, 1989, "Instability in a sand heap" *Phys. Rev. Lett.*, 69:44-46.

10. Laroche, C. ,S. Douady, S. Fauve,1990, "Convective flow of granular masses under vertical vibrations," *J. Phys. France*, 50:699-706.

11. Pak, H., R. Behringer, 1993, "Surface waves in vertically vibrated granular materials,", *Phys. Rev. Lett.*, 71:1832-1835.

12. Melo, F., P. Umbanhowar, H. Swineey, 1994, "Transition to parametric wave patterns in a vertically oscillated granular layer," *Phys. Rev. lett.*, 72:172-175.

13. Douady, S., S. Fauve, and C. Laroche, 1989, "Subharmonic instabilities and defects in a granular layer under vertical vibrations," *EuroPhys. Lett.*, 8:621-627.

14. Ahmad, K., I. J. Smalley, 1973, "Observation of particle segregation in vibrated granular systems," *Powder Tech.*, 8:69-75.

15. Knight, J. B., H. M. Jaeger, S.R. Nagel, 1993, "Vibration-induced size separation in granular media: The convection connection". *Phys. Rev. Lett.*, 70:3728-3731.

16. Vanel, L., A. D. Rosato, R. N. Dave, 1997,"Rise-time regimes of a large sphere in vibrated bulk solids," *Phys. Rev. Lett.*, 78:1255-1258.

17. Brone, D., F. J. Muzzio, 1996,"Size segregation in vibrated granular systems: A reversible process," *Phys. Rev. E*, 56:1059-1063.

18. Cundall, P. A., O. D. L. Strack, 1979, "A discrete numerical model for granular assemblies," *Geotechnique*, 29:47-65.

19. Walton, O. R., R. L. Braun, 1986, "Viscosity, granular-temperature, and stress calculations for shearing assemblies of inelastic, frictional disks," *J. Rheology*, 30:949-980.

20. Walton, O. R., 1993, "Numerical simulation of inclined chute flows of monodisperse, inelastic, frictional spheres," *Mech. Mater.*, 16:239-247.

21. Gallas, J., H. Herrmann, S. Sokolowski, 1992, "Convection cells in vibrating granular media," *Phys. Rev. Lett.*, 69:1371-1374.

22. Taguchi,Y-H.,1992, "New Origin of convective motion: elastically induced convection in granular materials," *Phys. Rev. Lett.*, 69:1367-1370.

23. Lee, J., 1994, "Heap formation in two-dimensional granular media," *J. Phys. A*, 27:L257-L262.

24. Rosato, A., Y. Lan, 1994, "Granular dynamics modeling of vibration-induced convection of rough inelastic spheres," *Proceeding of the First International Particle Technology Forum,* Denver, CO, pp. 446-453.

25. Grossman, E. L., 1997, "Effects of container geometry on granular convection," *Phys. Rev. E*, 56:3290-3299.

26. Wassgren, C. R., M. L. Hunt, C. E. Brennen, 1997, "Effects of vertical vibration on hopper flows of granular material," *Mechanics of Deformation and Flow of Particulate Materials, Proceedings ASCE Symposium*, Evanston, IL, pp. 335-348.

27. Lan, Y., A. D. Rosato, 1995. " Macroscopic behavior of vibrating beds of smooth inelastic spheres," *Phys. Fluids*, 7:1818-1831.

28. Luding, S., H. J. Herrmann, A. Blumen, 1994, "Simulations of two-dimensional arrays of beads under external vibrations: Scaling behavior," *Phys. Rev. E*, 50:2100-3108.

29. Dr. Maher Moakher developed the code as post-doctoral research associate with the Department of Chemical and Biochemical Engineering at the Rutgers University, New Brunswick, New Jersey.

30. Allen, M. P., D. J. Tildesley, 1987, *Computer Simulation of Liquids*, Clarendon Press, Oxford, U.K.

31. Mindlin, R. D., 1949, "Compliance of elastic bodies in contact," *J. Appl. Mech.*, 16:259-268.

32. Ravichandran, T. P., A. Mujumdar, C. Y. Wu, S. Watano, R. N. Dave, 1998, "Study of powder segregation during discharge from a vibrated hopper," Presented at AIChE 1998 Annual Meeting, November 15-20, Miami, Florida.

33. Brennen, C. E., S. Ghosh, C. R. Wassgren, 1996, "Vertical oscillation of a bed of granular material," *J. Appl. Mech.*, 63:156-151.